Marine Biology
January 2024, Volume 171 Issue 1 Pages 26 (22p.)
https://doi.org/10.1007/s00227-023-04346-6
https://archimer.ifremer.fr/doc/00866/97805/

The importance of niches in defining phytoplankton functional beta diversity during a spring bloom

Louchart Arnaud [1, 2, *], Lizon Fabrice [1], Debusschere Elisabeth [3], Mortelmans Jonas [3], Rijkeboer Machteld [4], Crouvoisier Muriel [1], Lebourg Emeline [1], Deneudt Klaas [3], Schmitt François G. [1], Artigas Luis Felipe [1]

[1] Laboratoire d'Océanologie et de Géosciences, Univ. Littoral Côte d'Opale, Univ. Lille, CNRS, IRD, UMR 8187, LOG, 62930, Wimereux, France
[2] Department of Integrative Marine Ecology, Stazione Zoologica Anton Dohrn, 80121, Naples, Italy
[3] Flanders Marine Institute, InnovOcean Campus, Jacobsenstraat 1, 8400, Ostend, Belgium
[4] Laboratory for Hydrobiological Analysis, Rijkswaterstaat (RWS), Zuiderwagenplein 2, 8224, Lelystad, The Netherlands

* Corresponding author : Arnaud Louchart, email address : arnaud.louchart@gmail.com

Abstract :

Ecological niches and beta diversity are fundamental concepts providing insight into the structure and functioning of marine ecosystems. Both concepts help in understanding how communities are distributed in different habitats and how marine ecosystems respond to environmental change. Here, the study brings a functional approach to the relationship between phytoplankton ecological niches and beta diversity. Phytoplankton community (from pico- to microphytoplankton) was addressed during a spring bloom of Phaeocystis globosa and diatoms, from the eastern English Channel (EEC) toward the southern North Sea (SNS) in 8 distinct water bodies, from late-April 2017 to mid-May 2017. An automated flow cytometer was used to discriminate phytoplankton by their optical properties at the single-cell level from continuous subsurface pumping marine waters, allowing the characterization of 11 phytoplankton functional groups (PFGs) from pico- to microphytoplankton. The spatial segregation of PFGs was performed from total abundance and Local Contribution to Beta Diversity (LCBD) calculations, from the most abundant to the marginal PFGs, through niche's overlap. Nanoeukaryotes (RedNano) associated with Phaeocystis globosa and picophytoplankton associated with Synechococcus spp. (OraPicoProk) were the less marginal PFGs. However, the low niche overlap between these groups revealed they have contrasting habitat affinity. While nanoeukaryotes prefer estuarine habitats or at the vicinity of an estuary, Synechococcus spp. was more likely along the coasts without freshwater influence. Picoeukaryotes with high chlorophyll-a content (RedPico III), coccolithophores (HsNano), and Pseudo-nitzschia-like (RedMicro I) were highly marginal revealing a patchy distribution. Finally, the beta regression predicted changes in community composition (i.e., LCBD values) influenced positively by temperature and the distance to the coast and negatively by salinity. The overall contribution of the PFGs to these changes (i.e., Species Contribution to Beta Diversity) was positively linked to their niche position and negatively related to their environmental tolerance.

Keywords : Beta diversity, Ecological niches, Flow cytometry, Spatial variability, Spring bloom

1. Introduction

Species distribution is the core of biodiversity research analyzing species and environmental interactions at different spatial and temporal scales. Nevertheless, the scale of variability of the distribution of a species depends, in the first place, on the abundance, physiology, size and metabolism of organisms and then, on the characteristics of the ecosystem and associated processes considered. In marine ecosystems, coastal and marginal seas represent a boundary between open ocean and continental ecosystems, being economically important as they represent between 22% and 43% of the estimated value of ecosystems services on Earth (Costanza et al. 1997). Hydrological, geochemical, geological and biological processes of coastal ecosystems are continuously influenced by natural (e.g. turbulence, tides, winds, rivers run-off) and direct/indirect anthropogenic pressures (e.g. eutrophication, topography modification, contribution to global change) which leads to changes in the structure and processes, according to the timing and spatial extent of these events. In highly hydrodynamic areas, such pressures can generate patches at meso- and sub-mesoscale and make it particularly challenging to assess and understand the temporal and spatial distribution of phytoplankton (Seuront et al. 1999; Lovejoy et al. 2001; Cullen et al. 2002).

In theoretical ecology, nine hypotheses are often used to describe the relation between distribution and species abundance (Gaston et al. 1997; Gaston and Blackburn 2007). Four hypotheses are related to data acquisition and data analysis while five are related to the ecology of species. Among the ecological hypotheses, habitat use is known to affect species occupancy and abundance because each species has its own niche and consequently may influence spatiotemporal variability of phytoplankton diversity. Species abundance related to their environment is often explained by species niche parameters (i.e. niche position and niche breadth). This concept is defined as the environmental space that a species can occupy according to their metabolic requirements and their abiotic parameters. To this, Hutchinson added the n-dimension feature in the fundamental niche where each dimension is represented by a factor of the environment (Hutchinson 1957). Consequently, spatiotemporal patterns in species diversity should be related to niche parameters. First, (Heino 2005) stated that niche hypothesis predicts that species having a marginal niche are less widely distributed and locally less common than species capable of occurring in average habitat conditions, defined by the average environmental parameters used in the study. Therefore, it is assumed that species having the broader niche (non-marginal niche) have a wider regional occupancy. Secondly, the spatiotemporal index for diversity estimation such as the Species Contribution to Beta Diversity (SCBD; Legendre and De Cáceres 2013) is related to niche position because species occurring in marginal habitats should occur in environmentally more restricted conditions than non-marginal species.

The identification and quantification of phytoplankton species is mainly based on morphology and processed by microscopy which often misses most cells below 5 µm (Rutten et al. 2005). Moreover, species occurring in the same community which have similar traits may reveal 'redundancy' in ecological functions (Salmaso et al. 2015). Consequently, using a trait based analysis focusing on individual phenotypes rather than species appears to be more relevant in understanding ecosystem functioning by avoiding this redundancy (Fontana et al. 2014). Grouping species together based on similar morphological, physiological and ecological features such as traits, defines functional groups (Litchman and Klausmeier 2008) and reflects a functional diversity within a community. Most of the traits used to characterize the functional groups are morphological and physiological traits and, if required, some taxonomical (Salmaso et al. 2015) and ecological information (e.g. silicifiers/calcifiers) can be

added. Recently, studies showed this morpho-physiological classification can be obtained using the optical features of particles (single-cell and colonies), covering most of the size-range of phytoplankton (1-800 µm), assessed by the "pulse shape-recording" automated flow cytometer (Fontana et al. 2014; Fragoso et al. 2019). In addition, recent study showed that the concept of phytoplankton niches can be applied on functional groups (Nagy-László et al. 2020). Based on the arguments exposed above, our study relies on the use of functional groups through the principle that functional diversity is more sensitive to pressure than taxonomic diversity.

In coastal areas, phytoplankton blooms often last from a week to one or two months. In coastal ecosystems particularly characterized by high hydrodynamics, current sampling strategies (discrete stations sampled weekly, fortnightly or monthly) can miss short-term events as well as the onset of blooms, local and/or sub-mesoscale patches and their spatial extension, which can lead to misinterpretations of their importance for trophic networks and biogeochemical cycles and to insufficient measures to deal with harmful events. The eastern English Channel (EEC) and the southern bight of the North Sea (SNS) are tightly connected areas of the two marginal seas (English Channel and North Sea) under the influence of Atlantic waters flowing from the West (Celtic Seas, the Atlantic eastern shelf waters) and from the North of the North Sea. Several rivers contribute to bring freshwater and nutrients into these areas which are mainly the Seine, the Somme (completed by five estuaries of decreasing flow northwards to the Strait of Dover), the Thames and the western Scheldt-Rhine-Meuse estuaries, which inputs form Regions Of Freshwater Influence (ROFI). The spread of riverine inflow depends on river flow, tidal and coastal currents, as well as on main winds, resulting, in French eastern English Channel coasts, to a brackish "coastal flow" (Brylinski 1991). The bottleneck of the Dover Strait, contributes to residual and tidal coastal currents flowing towards the North (both brackish coastal waters and offshore Atlantic waters; Sentchev and Korotenko 2005). In spring, phytoplankton biomass accumulates, benefiting from the winter nutrients stocks and the increase in light intensity and the de-coupling of grazers. Spring blooms in these systems are characterized by the Haptophyte *Phaeocystis globosa* representing up to 80% of the total biomass (Breton et al. 2000; Seuront et al. 2006; Aardema et al. 2019; Aubert et al. 2022), mainly along French, Belgian and Dutch coasts and is preceded, coupled to (Sazhin et al. 2007; Aubert et al. 2022) and followed by diatoms blooms (Schapira et al. 2008; Grattepanche et al. 2011). Notwithstanding phytoplankton blooms are highly documented and benefit from long-term regular monitoring at discrete stations (sampled fortnightly to monthly). The high hydrodynamical changing conditions experienced by these areas define different scales of variability that might be missed by reference monitoring approaches (Thyssen et al. 2008; Bonato et al. 2015, 2016; Louchart et al. 2020b) and thus, generate an alternance of patches of high and low abundance (Louchart et al. 2020b).

Recently, regular fortnightly monitoring on a discrete station in the EEC and SNS allowed a temporal study of the realized niche of *Phaeocystis globosa* (Karasiewicz et al. 2018). Nevertheless, in this highly hydrodynamical changing area under strong tidal forcing, tidal and haline fronts, ROFIs (Quisthoudt 1987; Brylinski et al. 1996; Brunet and Lizon 2003; Lacroix et al. 2004; Ruddick and Lacroix 2006), studying the niches on discrete monitoring points can be inadequate to capture the natural variability. Increasing the frequency of monitoring is necessary to have a more reliable view of the system across spatial and temporal scales (Derot et al. 2015). For this purpose, automated techniques were previously used to resolve spatial distribution of phytoplankton communities at high

temporal and spatial resolution during the spring blooms either in the EEC or in the SNS (Houliez et al. 2012; Bonato et al. 2015, 2016; Thyssen et al. 2015; Louchart et al. 2020a).

Here, we aimed at explaining phytoplankton beta diversity by considering niches at sub-mesoscale (< 10 km), on a functional diversity approach of the whole phytoplankton size-range (including picoplankton). The study considered the development of spring blooms of diatoms and *Phaeocystis globosa* from the eastern English Channel towards the Wadden Islands in the southern North Sea, and drifted northwards by both tidal and wind-induced currents (Sentchev and Korotenko 2005). We targeted the 2017 spring bloom sampled over one month (21 April 2017 to 18 May 2017) and three international and collaborative cruises (PHYCO-cruise, VLIZ-cruise and RWS-cruise, in the frame of the JERICO-NEXT European H2020 project). The sampling strategy of this survey consisted of 2 complementary approaches performed on each of the three cruises. First, the core of our survey relied on a high-frequency approach (continuous underway data) for measurements of temperature, salinity and cytometric groups. Then, a low-frequency approach was applied across 60 distributed stations over the entire study area. Sub-surface samples were collected on discrete stations for nutrients and phytoplankton microscopic identification and counting. These data were collected and used for interpretation of high frequency results. Our goals were: 1) to determine the optically-defined phytoplankton functional groups (PFG) that mostly influenced the composition of the different communities at each site, searching for their Local Contribution to Beta Diversity (LCBD), 2) to define phytoplankton niches by functional groups and 3) to establish the relation between the niche of the PFGs and the beta diversity.

2. Materials and methods

2.1. Cruise outlines

Samples were collected during three international collaborative cruises in 2017 (Figure 1) supported by French, Dutch and Belgian national and/or local projects (i.e. CPER MARCO and MSFD CNRS/INSU-MEMM/MTES convention for LOG in France and Monitoring Waterstaatkundige Toestand des Lands for RWS in the Netherlands). The international collaboration was carried out in the frame of the Joint European Research Infrastructure for Coastal Observatories-New EXpertise (JERICO-NEXT, H2020 INFRAIA) and LifeWatch (ERIC) European projects. The cruises started during well-established bloom conditions in the eastern English Channel before their spread in the southern North Sea waters. From April 21 to 30, 2017, the PHYCO cruise onboard the RV *Côte de la Manche* (CNRS-INSU, Artigas, 2017) focused on a round trip within the eastern English Channel (from the Seine River and Portsmouth to the Strait of Dover). Then, round-trips were carried out from French (EEC) and Belgian coastal waters (SNS) and the Scheldt-Rhine-Meuse plume to English coastal waters by the strait of Dover and the Thames dilution plume during the JERICO-NEXT/LifeWatch VLIZ cruise (8 to 12 May 2017) onboard the RV *Simon Stevin* (VLIZ). During the MWTL RWS cruise onboard the RV *Zirfaea* (15 to 18 May 2017), a round-trip started from the Rhine, Meuse and Scheldt and went towards the Wadden Islands and almost to the German Bight. In the three cruises, seawater was pumped continuously at 3 m depth through a circulation device and analyzed with an automated pulse shape-recording Flow Cytometer (PSFCM) to track and record phytoplankton cells and colonies every 10 min. In addition, continuous parameters were obtained by the thermosalinometer (SeaBird SBE21; PHYCO cruise) and FerryBoxes (4H-JENA engineering GmbH; VLIZ and RWS cruises). Three main French estuaries (Somme, Authie and Canche) and smaller estuaries by the Dover Strait

on one side and the western Scheldt – Rhine – Meuse ROFI on another side were both investigated twice. While the three French estuaries and the Dover Strait were investigated during the PHYCO cruise (20 to 21 of April) and during the VLIZ cruise (8 to 9 of May), the western Scheldt – Rhine – Meuse ROFI was investigated during the VLIZ cruise (11 to 12 May) and during the RWS cruise (18 of May).

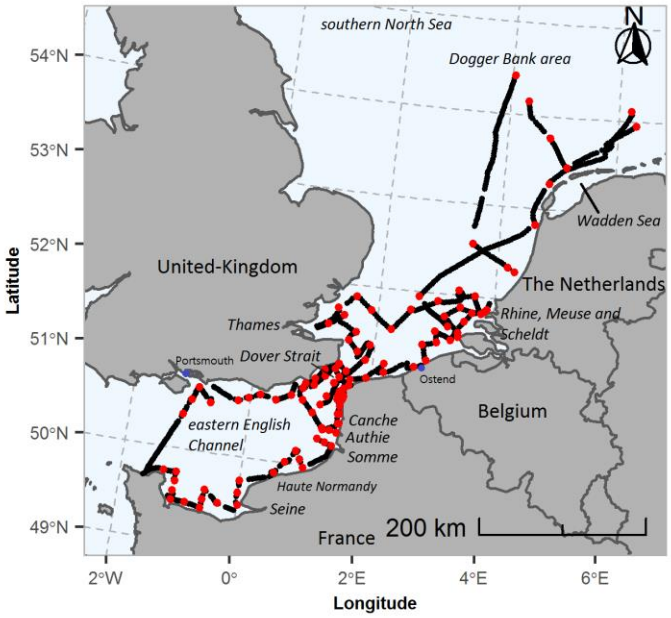

Figure 1: Studied area of PHYCO (CNRS-LOG), JERICO-NEXT/LifeWatch (VLIZ) and MWTL (RWS) cruises in the eastern English Channel (PHYCO and JN/LW cruises), southern North Sea and along the Wadden Islands (JN/LW and MWTL cruises) from April 21 to May 17, 2017. Black dots represent the continuous measurement recorded with the thermosalinometer, Ferrybox and the CytoSense flow cytometer. Red dots represent the discrete sampling stations investigated during the three cruises. A list of the abbreviations can be found in the supplementary material (Annex 1).

2.2. Discrete data

Samples for nutrient analyses were collected at 104 discrete stations (Figure 1, PHYCO cruise: 47, JERICO--NEXT/LifeWatch cruise: 43 and MWTL cruise: 14). For PHYCO cruise, samples were collected and directly frozen. For JERICO-NEXT/LifeWatch cruise, around 200 mL of seawater was filtered through a 47 mm, 0.2 µm cellulose-acetate filter for residual water. When the filter runs dry, 150 mL of filtered water is poured into a recipient and then stored at −24 °C. For MWTL cruise, samples were filtered onto Whatman GF/F filters and kept frozen at -18°C until analyses. Analyses of ammonium ($NH4^+$), nitrite (NO_2^-), nitrate (NO_3^-), phosphate (PO_4) and silicates (SiO_3) were processed by each institute for the respective cruise (CNRS-LOG for PHYCO cruise, VLIZ for JERICO-NEXT/LifeWatch cruise, RWS for MWTL cruise). Nutrients were analyzed according to (Aminot and Kérouel 2004) in an SEAL AutoAnalyzer 3 High Resolution (SEAL AA3 HR; Seal Analytical, Wisconsin, USA) for PHYCO cruise. Detailed procedure for the RWS can be found in Aardema et al. (2019) and for VLIZ in Mortelmans et al. (2019). In the present study, single nutrient forms were not presented as potentially subjected to variation due to methodology (sensor, storage duration). Nevertheless, ratios between nutrients must not be impacted as the chemical analysis *per se* remained identical across nutrients.

2.3. Continuous underway data

2.3.1. Hydrological parameters

The high-resolution environmental data set included temperature, salinity, bathymetry and distance to the coast. Temperature and salinity were recorded every 15 s by a thermosalinometer (SeaBird SBE21; PHYCO cruise) or Ferryboxes (4H-JENA engineering GmbH; JERICO-NEXT/LifeWatch and MWTL cruises). The data were averaged every 10 min to match phytoplankton data set. Bathymetry was extracted from the General Bathymetry Chart of the Ocean (GEBCO). An R script was written to extract the distance from the coast of each record. We used gdistance function (*gdistance* package; van Etten 2017) to calculate the shortest distance between each pair of latitude-longitude associated to thermosalinometer records and a 10 m resolution shapefile obtained from rnaturalearth package (Massicotte et al. 2023). To obtain accurate measure of the distance to shore, the coordinates reference systems was set common between the shapefile and the sampling dataset prior the calculation. Sampling was processed from 20 m to 136 km off the coast.

2.3.2. Automated flow cytometry

A second data set included phytoplankton abundance per phytoplankton functional group defined by flow cytometry analysis, using a CytoSub and/or a CytoSense (Cytobuoy b.v., the Netherlands) which are automated pulse shape-recording flow cytometers (PSFCM). The PSFCM is a powerful technique to analyze, count and characterize single-cells and colonies, *in vivo* and at high frequency, from 1 to 800 µm width and up to a few millimeters' length. The PSFCM records a "pulse shape" (Dubelaar et al. 1999) derived from optical features of each single particle, after passing through a solid-state Sapphir laser (Coherent Inc, 488 nm, 50 mV), providing morphological and optical traits that reflect actual physiological traits (Pomati et al. 2013; Fontana et al. 2018; Fragoso et al. 2019). The size of particles is addressed and derived from the forward scatter (FWS) after bead correction and is collected by a PIN photodiode. Internal (e.g. size of the vacuole) or external (e.g. presence of mineral scales) compositions are addressed by the sideward scatter (SWS). In addition, three types of fluorescence are recorded: red fluorescence (FLR; emission: 668–734 nm), orange fluorescence (FLO; emission: 604–668 nm) and yellow fluorescence (FLY; emission: 536–601 nm). Both fluorescence and SWS are recorded by a set of photomultipliers. We set up a low trigger level on the red fluorescence (range between 10 to 14 mV in the present case) to separate phytoplankton from non-autofluorescent particles (Thyssen et al. 2015). Finally, the sensor was equipped with a camera, supplying pictures of the largest cells > 20µm allowing coarse taxonomical recognition (Dugenne et al. 2014; Pereira et al. 2018). The CytoClus software (Cytobuoy b.v., the Netherlands) allowed the visualization and characterization of the groups by the combination of features (Length, Total, Maximum) of the five signals recorded (FWS, SWS, FLR, FLO, FLY) mapped in 2-dimensions dot plots (cytograms). The amplitude and the shape were used to discriminate different optical groups. Particles sharing similar optical properties (i.e. features and signals) were gathered together using the CytoClus software (CytoBuoy b.v.) by manually gating a bulk of similar particles. According to the definition given by (Reynolds 1997), phytoplankton sharing similar morphological, physiological and/or ecological properties such as calcifiers (HsNano) or silicifiers (diatoms) can be grouped together to form what is called Phytoplankton Functional Groups (PFGs). In our case, the different phytoplankton cytometry-defined groups were labelled from their optical characteristics, according to the criteria of the standardized vocabulary (Thyssen et al. 2022). We discriminated 6 main phytoplankton groups traditionally

observed according to their size and fluorescences (red, orange and yellow): OraPicoProk, RedPico, RedNano, OraNano, HsNano and RedMicro (Thyssen et al. 2022). Moreover, SideWard Scatter (SWS) of the PFG and their fluorescence intensities, contributed sometimes to characterizing some sub-groups.Therefore, we could refine 4 subgroups in the RedPico (RedPico I, RedPico II, RedPico III and RedPico IV), 3 subgroups in the RedNano (RedNano I, RedNano II and RedNano III) and 2 subgroups in the RedMicro (RedMicro I and RedMicro II). In this study we infer the RedNano groups to *P. globosa* single cells (Brussaard et al. 1996; Rutten et al. 2005; Bonato et al. 2015) after testing the relation between RedNano groups sorted by the PSFCM and *P. globosa* counts by microscopy (Louchart et al. 2020a). We also processed images focusing on a targeted area of the cytograms corresponding to microphytoplankton, for subgroup visual validation of inferred taxa.

The size of particles was calibrated by a set of beads of 3 and 10 µm, which helped us to define three phytoplankton groups according to the size: Picophytoplankton (< 1-3 µm), Nanophytoplankton (3-20 µm) and Microphytoplankton (> 20 µm). Following Bonato et al., (2015), we applied a correction factor (Eq. 1) to estimate the size of each particle (Eq. 2) to finally provide an average estimation of cell size within each population.

$$\text{Correction factor} = \text{Real beads size} / \text{Measured beads size} \quad \text{(Equation 1)}$$

$$\text{Estimated particle size } (\mu\text{m}) = \text{Measured particle size} \times \text{Correction factor} \quad \text{(Equation 2)}$$

2.4. Data analysis

2.4.1. Water bodies

Within the whole study area, we defined water bodies from high frequency data (temperature, salinity, bathymetry and distance to the shore) by a three-step procedure: 1) computation of a Euclidean distance matrix on standardized data (temperature, salinity, distance to the shore and bathymetry). 2) Processing a hierarchical agglomerative classification by the Ward method. 3) Getting the optimal number of areas when the highest Calinski-Harabasz criterion value was obtained. A similar procedure referring only to physico-chemical features has also been described by Louchart et al. (2020b).

2.4.2. Local and Species Contribution to beta-Diversity

Our three cruises defined a set of phytoplankton functional groups combined into phytoplankton communities. First, we ran the Local Contribution to Beta Diversity in order to highlight the spatial changes in the community functional composition (Legendre and De Cáceres 2013). Briefly, the LCBD is a comparison of the uniqueness of each site to beta diversity. A site with a common composition would have a LCBD value close to 0. High LCBD values may indicate sites characterized by high conservation values or degraded and poor site in terms of richness and abundance (Legendre and De Cáceres 2013). High values may also correspond to particular ecological conditions or results from the disruptive effect of invasive organisms. Thus, beta diversity is particularly useful for conservation measures and marine policy management (e.g. European Marine Strategy Framework Directive, OSPAR convention). The analysis considers richness and the abundance of each biological element per site. Therefore, it is particularly suitable for high frequency datasets even though we did not consider species but functional groups. Prior to the analysis, the data were transformed by the Hellinger transformation. Briefly, the Hellinger transformation is the square root of sample total standardized data. This transformation is strongly

recommended for abundance data and especially in the use of the LCBD (Legendre and De Cáceres 2013). The cytometry-defined functional groups were found in almost each location except for *Pseudo-nitzschia* spp for which the absence was defined as null abundance. HsNano, another marginal PFG (PFG restricted to a limited range of habitat within the study area), was detected mostly everywhere but its abundance was especially very high near the Dogger Bank. Therefore, the variability in LCBD depended only on the relative abundance of each ecological unit (defined here as a PFG) in each site and should highlight changes in the community structure (Rombouts et al. 2019). The computation of the β-diversity provided also the Species Contribution to Beta Diversity (SCBD) which is the degree of variation of individual species (in this case, of a phytoplankton functional group) across the study area. Calculations of both LCBD and SCBD were carried out using the *beta.div* function of the *adespatial* package in R (Dray et al. 2022).

Community changes between the water bodies were detected by averaging values of the total LCBD for each water body. LCBD values amongst areas were tested by Kruskal-Wallis test and Dunn pairwise test with a Bonferroni correction. The calculation of the SCBD for each water body allows the identification of the PFGs which contributed the most to the changes in term of community composition.

2.4.3. Niche parameters

To determine the relation between PFGs and the environment at a fine resolution scale, we calculated the niche position and niche breadth using the Outlying Mean Index (OMI), by following the procedure described by Dolédec et al. (2000), adapted to PFGs. This is a multivariate index which allows the quantification of niche parameters and explains the variability of species to a selected set of environmental factors (Dolédec et al. 2000; Karasiewicz et al. 2017). Here, niche parameters were established for high resolution phytoplankton datasets (i.e. abundance recorded by the automated flow cytometer) and calculated using the high-resolution abiotic dataset (i.e. temperature, salinity, distance to the shore and bathymetry). Nutrients were not included in this analysis as the OMI analysis does not allow the use of two data sets with different resolutions. The OMI provides the inertia, the Outlying Mean Index (OMI), the tolerance and the residual tolerance. The significance level is obtained for each PFG. The inertia represents a quantification of the influence of the environment on the niche separation of the PFG and contributes to the characterization of the global niche overlap of the PFGs. The OMI or the marginality represents the deviation of the average position of a PFG to center of the analysis. Therefore, a PFG that shows low values of OMI has non-marginal niches and thus occurs in common habitats (i.e. everywhere). On the contrary, a PFG that shows high values of OMI has marginal niches and therefore, occurs in specific habitats. The tolerance represents the spatial and temporal variance of the OMI of a PFG across the given gradient of environmental parameters. Thus, a PFG that shows low values of tolerance has a narrow niche breadth whereas the PFG that shows high values of tolerance has a wide niche breadth. Finally, the residual tolerance evaluates the suitability of the environmental variables used to define the species niches. The statistical procedure is detailed in Dolédec et al. (2000). The OMI analysis was conducted using the niche function of the *ade4* R package (Dray and Dufour 2007). Exact p-values are reported to minimize false positive results. Significant threshold is however set up at $P < 0.001$, based on 1000 random permutations data. Until recently, the usual procedure to characterize niche position and niche breadth per subset (subniche) was to process several OMI analyses, one per subset. Nevertheless, this method assumed a unique origin of each subset of environmental conditions. In the case of different environmental conditions, the niches' positions vary between the subsets, thus the use of several OMI

cannot rely accurately a comparison of the subsets. For this purpose, the WitOMI analysis developed by Karasiewicz et al. (2017) defined a common origin for the overall analysis and an origin for each subset. The calculation of the WitOMI was carried out by the subniche function of the R package *subniche* (Karasiewicz et al. 2017). Both marginality and tolerance were obtained for the OMI and WitOMI analysis. The marginality is defined as the distance between the mean habitat conditions used by the functional unit and the mean habitat conditions over the entire studied area. The tolerance corresponds to the niche breadth which refers to the variability of the environment used by the functional units. In addition, the residual tolerance is calculated and represents the part of the variance which is not explained by the environment.

The last procedure of the niche analysis at small scales assesses how the groups are arranged between them. For this purpose, we estimated the niche overlap based on the method of Broennimann et al. (2012). This procedure uses a kernel density estimation (kde function of the *ks* package for R, Chacón and Duong 2018) weighted by the abundance of each group to create an occurrence density for each phytoplankton group. The coordinates of the kernel were set by the first two axes of the OMI analysis following the procedure of Hernández Fariñas et al. (2015). We set our space grid (r x r) for the kernel with r = 100. The comparison between two phytoplankton groups were then assessed by the Schoener D metric which quantifies the percentage of commonness between groups (Schoener, 1970). The overlap statistic (Eq. 3) is given by:

$$\text{Equation 3: } D_{1,2} = 1 - \frac{1}{2}\sum_{ij} p_{1ij} - p_{2ij}$$

Where p_{1ij} is the relative abundance of group 1 at the site ij and p_{2ij} is the relative abundance of the group 2 at the site ij.

Additionally to niches analysis estimated by high resolution approach, a 1-dimension Kernel Density Estimation (KDE) was also processed for each nutrient ratios and each phytoplankton group based on the discrete sampling. This analysis provides the observed distribution of each PFG for continuous data. In our case, the KDE provides the affinity of each phytoplankton group for each nutrient during this snapshot of mid-spring 2017.

2.4.4. Deterministic model

Finally, we used the beta regression to model the β-diversity indices responses (LCBD and SCBD) with the environmental parameters and the niche features. This method is particularly suitable to model the distribution of response variables within the interval [0;1] such as the LCBD and SCBD. We processed the beta regression and the logit link function in two separate models. First, the LCBD was modeled with 4 environmental parameters as predictors (temperature, salinity, bathymetry and the distance to the shore). We used only these 4 environmental parameters as their high recording frequency matched the spatial resolution of the LCBD. The second model used the niche parameters (niche position and niche breadth) as predictors of the SCBD. To account for spatial autocorrelation, we consider latitude and longitude as fixed effect in LCBD model. In the SCBD, as data were computed at the water body level, it was not possible to use latitude and longitude as fixed effect. Thus, water body was considered as the fixed effect. Both models obtained (LCBD and SCBD as response) produced a pseudo-R^2. The calculation of beta regression was processed in R using the *betareg* package (Cribari-Neto and Zeileis 2010).

3. Results

3.1. Hydrology

Temperature, salinity, bathymetry and distance to shore were variables recorded continuously. Silicates, nitrates, nitrites and phosphate were obtained at discrete stations. Continuous environmental parameters were used to define water bodies and were plotted on a TS diagram (Figure 2A) at fine scales whereas nutrients were used to supplement niche analyses. Mean temperature was 11.36 ± 0.68 °C. Minimum temperatures reached 9.83 °C the 15 of May near the northern point sampled during the survey whereas the maximum was 15.24 °C reached the 18 of May near the southern Dutch coast. Mean salinity was 34.01 ± 0.80. Minimum salinity was 29.33 and recorded near the coast and southern to the Meuse estuary the 18 of May. Maximum salinity reached 35.30 and was recorded on the way to transect to the farthest sampling station of the North Sea.

The 95th percentile for nutrients (µM) ranged from [0.03; 19.94] for ammonium, [0.03; 49.94] for Nitrates, [0.02;1.96] for Nitrites, [0.31;69.04] for Silicates, and [0.02;6.02] for Phosphate. Therefore, ninety-fifth percentile were [3.41;113.30] for N:P ratio, [1.11;115.41] for Si:P and [0.04;3.47] for Si:N. Maps of log10 of nutrients ratios can be found in the supplementary material (Appendix 2). In the present study, salinity was negatively correlated to nutrients concentrations (ρNO_3^- = -0.58; ρNO_2^- = -0.38; ρNH_4^+ = -0.37; ρSiO_3 = -0.37; N = 104, all significant at $P < 0.001$). On the opposite, temperature was positively correlated to nutrients concentrations (ρNO_3^- = 0.38; ρNO_2^- = 0.49; ρPO_4 = 0.45; ρNH_4^+ = 0.62; ρSiO_3 = 0.42; N = 104, all significant at $p < 0.001$). Finally, the distance to the shore was positively and significantly related to nutrients ρNO_3^- = 0.33; ρSiO_3 = 0.29; ρPO_4 = 0.47; N = 104, all significant at $P < 0.05$) which is coherent with the pre-bloom situation as nutrients close to the coasts are at high level because they have not been consumed yet by plankton.

3.2. Water bodies

The amplitude of the four variables recorded at high frequency (temperature, salinity, distance to the shore and bathymetry) supported the fact that several water bodies were crossed during the three cruises as evidenced by previous studies (Bonato et al. 2015; Aardema et al. 2019). While the Temperature-Salinity (TS) diagram alone was not able to discern the eight water bodies (Figure 2A), mapping the water bodies revealed their location in the study area (Figure 2B). Water body (WB) 8 was the most brackish (mean: 31.45 ± 0.68) and warmest WB (mean: 14.31°C ± 0.57) of the study area. It was located nearby the shore and corresponded to the brackish water of Northern Dutch estuaries and the Texel inlet by mid-May. Surrounding WB8, WB6 was the second warmest WB (mean: 12.82°C ± 0.44) with intermediate values of salinity (mean: 33.41 ± 0.66), bathymetry (mean: -21m ± 6) and distance to the shore (mean: 21km ± 13). It was mainly located at the vicinity of brackish waters of the SNS (Inlets between Texel and Vlieland and northern WRM). Brackish salinity (mean: 33.09 ± 0.47) was also observed in WB4. It was a shallow water bodie (mean: -17m ± 7) located nearby the coasts of the SNS and EEC during the whole period from mid-April to mid-May. WB4 corresponded therefore to coastal waters of the EEC and SNS influenced by freshwater inputs (Bay of Seine, Bay of Somme, southern WRM and connections between the Wadden Sea and the SNS). WB2 corresponded as well to coastal waters of the EEC and SNS (also including Thames plume) but it was less influenced by freshwater inputs than WB4 as average salinity was 34.39 ± 0.27 (Appendix 3). Water bodies 1 and 3 were characterized by similar salinity (respectively mean: 34.33 ± 0.37 and 34.42 ± 0.36), temperature (respectively mean: 10.96°C ± 0.34 and 10.92°C ± 0.23) and distance to the shore (respectively mean: 18 km ± 10 and 19 km ± 11). While WB3 was more likely found in the middle of the EEC,

probably resulting of Atlantic waters flowing towards the North Sea, WB1 corresponded to transient waters between coastal waters (WB2) and offshore waters (WB3). WB5 was slightly warmer (mean: 11.47°C ± 0.53) and saltier (mean: 34.92 ± 0.33) than WB3. WB5 could be characterized as an extension of WB3 in the SNS after a lag of 15 days. Finally, WB7 had high salinity (mean: 34.49 ± 0.05) but the coldest waters (mean: 10.24°C ± 0.27) and the farthest waters from the shore (mean: 110km ± 16). This WB was the northernmost of the study area, located at the vicinity of Dogger Bank, and was sampled only by mid-May

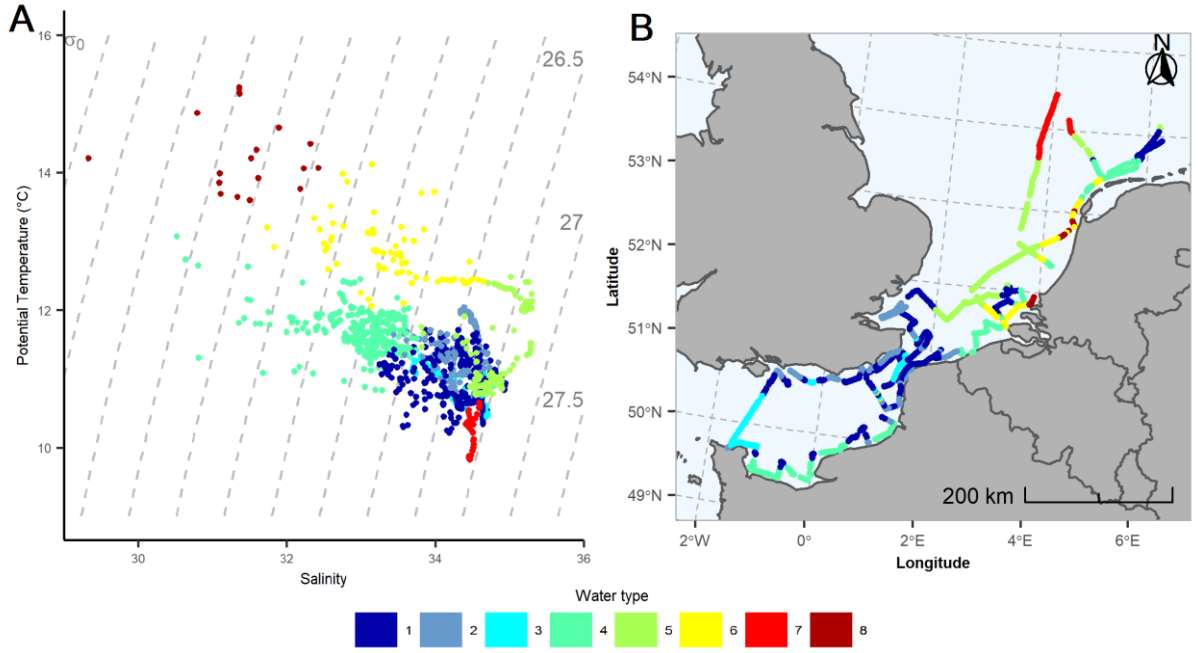

Figure 2: Water bodies discriminated from temperature, salinity, distance to the shore and bathymetry. A. TS diagram. B. Location of the eight water bodies.

3.3. High frequency flow cytometry

Up to 11 phytoplankton functional groups (PFG) were characterized during the 3 cruises. According to the correction size's formula provided by Bonato et al. (2015) and the common vocabulary described in Thyssen et al., (2022), we could characterize 4 picophytoplankton (including picocyanobacteria), 5 nanophytoplankton (including *Phaeocystis globosa* single-cell life stages) and 2 microphytoplankton groups larger than 20 µm (RedMicro I identified as *Pseudo-nitzschia* cells and the rest of Microphytoplankton labelled as RedMicro II) on the cytograms (Appendix 4). Size ranged from 1.99 ± 0.45 µm for OraPicoProk (*Synechococcus)* to 33.45 ± 10.25 µm for Microphytoplankton (Appendix 5). A strong spatiotemporal heterogeneity in phytoplankton distribution was evidenced (Figure 3). The overall most abundant groups exhibited up to 10^5 cell cm^{-3} including RedPico II (max: 1.51 10^5 cells cm^{-3}) and RedNano II (max: 1.29 10^5 cells cm^{-3}). There was nevertheless high heterogeneity in the abundance as RedPico II was 28 to 43 times more abundant in eastern English Channel than in southern North Sea. There was less heterogeneity in the abundance of RedNano II as there was only 2.5 times more cells in the brackish water than in offshore waters. The less abundant groups never exceeded 1.00 to 3.00 10^3 cells cm^{-3}, they were OraNano(max: 2.72 10^3 cells cm^{-3}) and RedMicro II (max: 9.40 10^2 cells cm^{-3}). Some PFGs sometimes exceeded 10^4 cell cm^{-3}: OraPicoProk (max: 1.47 10^4 cells cm^{-3}), RedPico I (max: 9.72 10^4 cells cm^{-3}), RedPico II RedPico III (max: 2.03 10^4 cells cm^{-3}) and HsNano (max: 2.03 10^4 cells cm^{-3}). RedNano PFGs (RedNano I,

RedNano II and RedNano III) were the dominant PFGs in the Strait of Dover and in French EEC waters under direct influence of Somme, Authie, Canche estuaries ("coastal flow"), in the Thames plumes as well as along the Belgian coast, in the Rhine, Meuse and Scheldt (ROFI) and along the Wadden Islands (SNS). They contributed to more than 50 % of the total abundance and often reached up to 2.00 10^4 cells cm^{-3}. A Spearman rank correlation on discrete stations of the PHYCO and MWTL cruises gave a strong and significant correlation (ρ = 0.75, N = 65, P < 0.0001) between the RedNano PFGs combined together and the microscopy counts of *Phaeocystis*. In WB 4, 6 and 8 (coastal waters influenced by ROFI, vicinity of brackish waters of SNS, brackish waters of SNS, respectively), we also characterized a group composed of a pulse shape with symmetric and narrow cells and two symmetric chloroplasts. According to the images obtained by the camera mounted on the flow cytometer (see description in (Pereira et al. 2018), the group labelled RedMicro I was *Pseudo-nitzschia* spp. Nevertheless, low but significant Spearman rank correlation was found for this group between the PSFCM and the microscopic counts (ρ = 0.39, N = 65, P < 0.0001; (Louchart et al. 2020a). OraPicoProk and RedPico (RedPico I, RedPico II and RedPico III) were the most dominant PFGs along the English coasts (except the Thames ROFI where RedNano PFGs were the most abundant groups), the Haute-Normandy coast and the Bay of Seine in the EEC and in offshore waters of the SNS, reaching up to 90% of the total abundance (Figure 3).

Spatial overlapped areas between the PHYCO and VLIZ cruises and then, VLIZ and RWS cruises, revealed also the short-term spatiotemporal phenology of phytoplankton groups, particularly nanoeukaryotes. Over fifteen days between the two investigations of the French EEC under estuarine influence (the absolute and relative abundance of RedNano II increased from April to May. In the second area of overlap (Rhine-Meuse-Scheldt plume area), the nanoeukaryotes dominance shifted from RedNano II to RedNano I in 6 days. The location of high abundance of nanoeukaryotes and Spearman rank correlation results connected to existing literature therein suggest that we have detected the *in situ* phenology of *Phaeocystis globosa* resulting in succession of RedNano II (diploid morphotype, stage of bloom initiation), RedNano III (free colonial cells, stage of bloom expansion) and RedNano I (haploid morphotype, stage of senescent bloom and winter morphotype) groups.

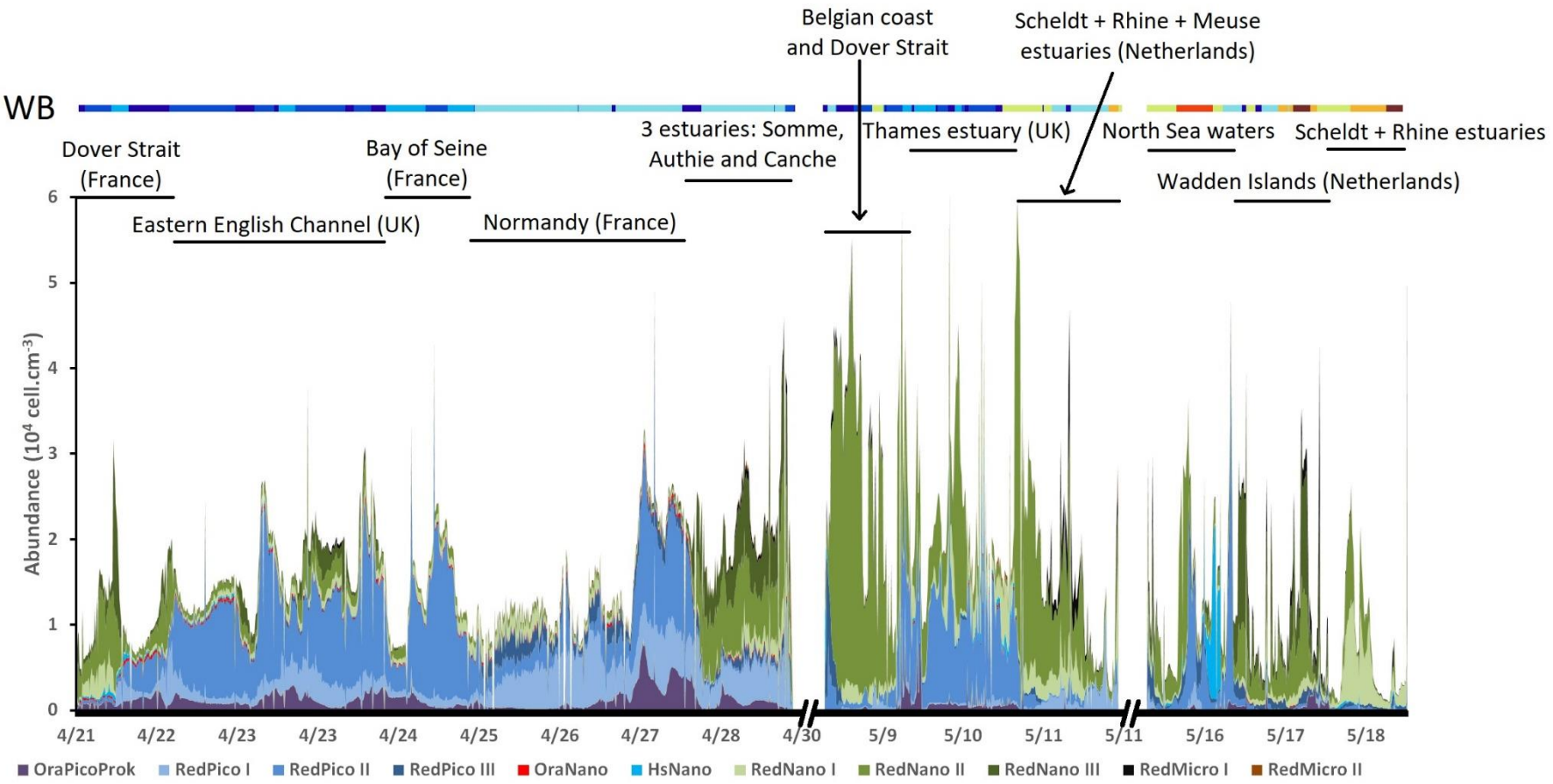

Figure 3: Spatio-temporal distribution of the phytoplankton functional groups sorted by the automated pulse shape-recording flow cytometer during the PHYCO cruise (04/21 to 04/30), the VLIZ cruise (05/08 to 05/11) and the RWS cruise (05:15 to 05/18), and corresponding Water Bodies (WB).

3.4. Local and Species Contribution to beta-Diversity

The sites with high and statistically significant values of LCBD (Figure 4) corresponded to spatial and/or temporal changes or turnover in the PFG assemblage's composition. During the whole sampling period, 6.1 % of the sites showed values of LCBD > 1.1953 10^{-3} displaying spatial and/or temporal heterogeneous breakdown of the LCBD index. High values formed 7 LCBD "hot spots": in some locations of the Bay of Seine by the end of April, in some locations of both French and Belgian SNS coasts by early May, by the Scheldt-Rhine-Meuse ROFI, at the mouth of Texel inlet and in a spot of offshore waters of the North Sea sampled at mid-May (Figure 4). The sites of significant LCBD values in the Bay of Seine (WB4; Coastal waters influenced by ROFI) were attributed to the large dominance of the RedPico II group. In the Belgian Coastal Zone (BCZ; WB2; Coastal waters + Thames Plume) by early May, the significant high values of LCBD were located at the vicinity of the Ostend harbor and attributed to the increase in RedMicro I abundance. In the western Scheldt, Rhine and Meuse ROFI and at the vicinity of Texel inlet (WB6 and WB8; Vicinity of brackish waters and Brackish waters, respectively), the high significant LCBD values were explained by the increase in the RedNano I contribution to the total abundance. Finally, central North Sea waters (at the Northern limit of the SNS; WB7; Vicinity of Dogger Bank) exhibited also high values of LCBD and corresponded to a large contribution of the HsNano group to the total abundance (Figure 4).

Five PFGs were characterized by a SCBD value above 10%: RedPico II (25%), RedNano II (17%), RedPico I (17%), RedNano III (13%) and RedNano I (10%). They followed a spatial segregation between English coasts and the Rhine-Scheldt-Meuse-Seine ROFIs, the French EEC "Coastal flow" and along the Wadden Islands. The latter areas were dominated by RedNano I, RedNano II and RedNano III. Moreover, the high and significant LCBD values were sparsely distributed within these areas (Figure 4). Consequently, the three RedNano groups mentioned above were strongly related to the atypical composition identified during this period due to their remarkably high abundance. The corresponding patchy and scarce areas were separated by large areas with low values of LCBD,mainly along the Haute Normandy coasts, the French coast of the North Sea and the Belgian Coastal Zone, apart the vicinity of Ostend harbor. None of the PFGs were dominant in these areas.

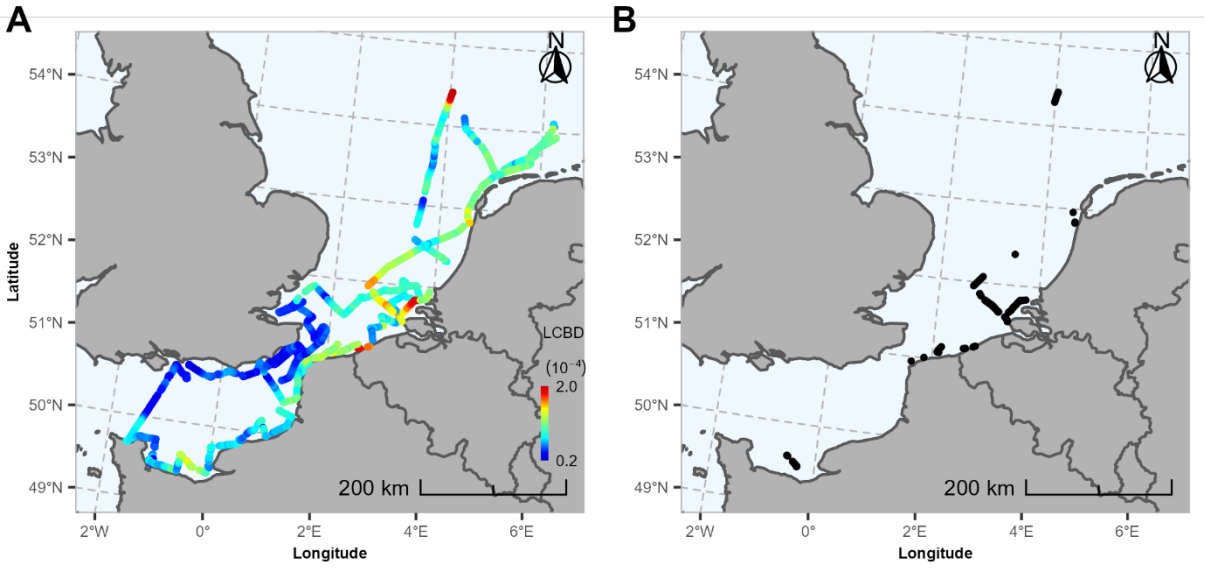

Figure 4: A) Map of the LCBD index values calculated on the abundance of phytoplankton functional groups defined by PSFCM. B) Location of significant LCBD values.

3.5. LCDB and SCBD per Water body

LCBD values made possible to address the extent of community changes across water bodies at high resolution. To help identify differences in community composition in relation to environmental variables, LCBD values were averaged per water bodies. A Kruskal-Wallis and Dunn pairwise tests detected significant differences (Kruskal-Wallis test, $H = 473.06$, $df = 7$, $P < 0.0001$) in the community composition through the LCBD values between the different water bodies (Figure 5). The lowest values of LCBD were found between water bodies 1, 2 and 3 spread on several offshore and coastal areas which, in turn, were slightly lower than the water body 4 corresponding to coastal waters influenced by ROFI (Figure 5). In the southern North Sea, the values of LCBD were significantly different between water bodies 5, 6 and 8 (Offshore waters of SNS, Vicinity of brackish waters, Brackish waters, respectively). LCBD of water body 7 (Vicinity of Dogger Bank) was not significantly different from water body 5 and water body 8 but lower than water body 6 which showed the highest LCBD values of all. The high and significant LCBD represented 19% of the sites of WB 7 (vicinity of Dogger Bank), 10% in WB 5 (Offshore waters of the SNS), 5% in WB 8 (Brackish waters between Texel and Vlieland), 3% in WB 4 (Coastal waters influenced by ROFI), 2.6% in WB 1 (Transient water between offshore waters and coastal waters) and 0.3% in WB 2 (Coastal waters + Thames plume).

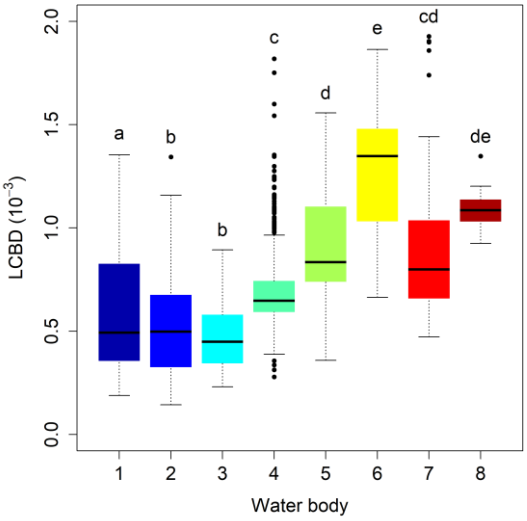

Figure 5: Boxplot of the LCBD values in each water body and their relations after Kruskal Wallis and Dunn pairwise tests with Bonferroni correction. Letters report the results of all pairwise comparison among the different water bodies.

The calculation of the SCBD amongst water bodies gave the contribution of each PFG to the beta diversity for each water body. PFGs contributed unequally to the SCBD (Figure 6). OraPicoProk showed the highest contribution (19%) to beta-diversity in water body 8 and the lowest in water body 5 and 7 (1% in both WB).

OraNano and, to a lesser extent, RedPico III, showed low contribution to the SCBD in most water bodies. RedNano I contributed the most to SCBD in water bodies 5 and 6 (27% and 29% of the total SCBD respectively). RedNano III showed its highest contribution to beta diversity in water bodies 5, 6 and 8 (23%, 25% and 29% respectively) while it was co-dominant with RedPico I, RedPico II and RedNano II group in the water bodies 1,2,3 and 4. In water body 7, there was a high contribution to beta diversity for the HsNano (44%). RedMicro II contributed up to 6.99 % to the beta diversity.

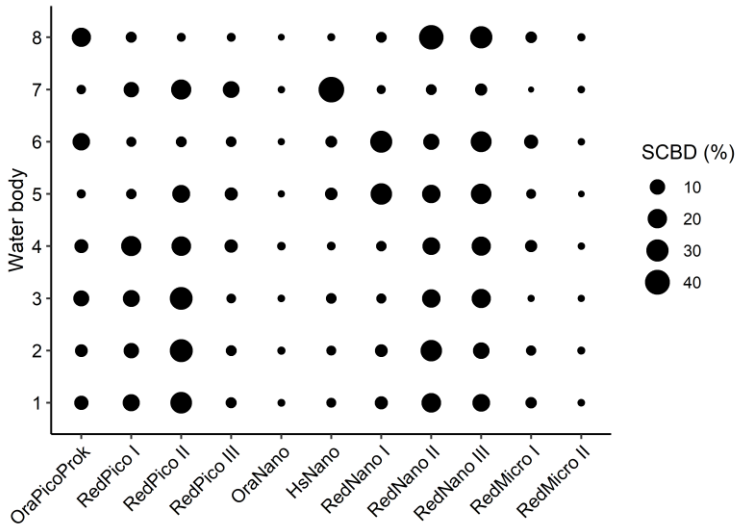

Figure 6: Species Contribution to Beta Diversity (SCBD) of each of the 11 phytoplankton functional groups among the eight water bodies. SCBD is expressed as the percentage of the contribution of a species j to the overall beta diversity in a given water body. The eleven PFGs are OraPicoProk, RedPico I, RedPico II, RedPico III, OraNano, HsNano, RedNano I, RedNano II RedNano III RedMicro I and RedMicro II..

3.6. Niche analyses

The global test of the average marginality of the PFGs obtained by the OMI analysis was significant, indicating the influence of the environment on phytoplankton community structure (Monte Carlo test, $p < 0.001$). All the PFGs showed a significant deviation of their niche from the origin (table 1). The 2 first axes of the OMI analysis represented 95% of the total variance with 55.2% of the total inertia explained by the first axis and 39.8% by the second axis (Figure 7). Axis 1 was explained by environmental parameters whereas axis 2 was explained by spatial gradients (offshore-inshore, East-West, North-South).

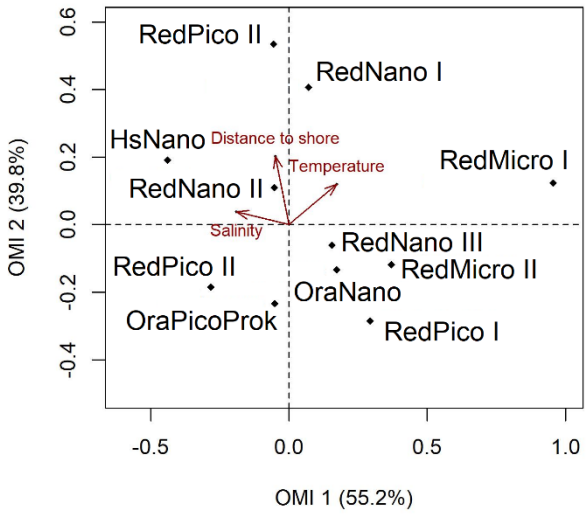

Figure 7: Outlying Mean Index (OMI) analysis of the eleven phytoplankton function groups (PFGs) characterized by automated pulse shape-recording flow cytometry according to the four continuously-recorded environmental parameters. Bathymetry was removed from the plot as it was not significantly involved in the analysis.

The table 1 summarizes the results of the niche analysis. For each PFG, the inertia, the Outlying Mean Index (OMI), the tolerance and the residual tolerance were obtained. The significance level was obtained for each PFG. Briefly, low marginality (OMI values < 0.10) was found for common and widespread PFGs (e.g. RedNano II, RedNano III and OraPicoProk) while high marginality (OMI values > 0.25) was reported for localized PFGs (e.g. RedPico III, HsNano and RedMicro I). The lowest tolerance was found for OraPicoProk and RedPico II while the highest tolerance was obtained for RedMicro I and HsNano PFGs.

Table 1: Niche parameters of the phytoplankton functional groups characterized in this survey.

PFG	Inertia	OMI	Tolerance	Residual Tolerance (%)	P-value
OraPicoProk	3.50	0.08	0.43	85.5	0.000999
RedPico I	3.21	0.17	1.35	52.6	0.000999
RedPico II	3.53	0.11	0.87	72.0	0.000999
RedPico III	6.21	0.30	1.62	69.0	0.000999
OraNano	3.62	0.07	1.09	68.0	0.000999
HsNano	6.03	0.28	3.33	40.1	0.000999
RedNano I	4.81	0.18	1.25	70.3	0.000999
RedNano II	4.05	0.02	1.43	64.2	0.000999
RedNano III	3.65	0.03	1.83	49.1	0.000999
RedMicro I	5.37	0.92	2.93	28.2	0.000999
RedMicro II	4.00	0.16	2.07	44.3	0.000999

Six patterns of PFGs emerged from the Kernel Density Estimation plots of nutrient preference (Figure 8) from discrete stations. OraPicoProk was likely found in areas with N:P > 16, Si:P < 16 and Si:N < 1. Then, RedPico I and RedPico II were preferentially observed in areas with N:P > 16, Si:P = 16 and Si:N < 1. RedPico III, OraNano, RedMicro I and RedMicro I were likely observed in areas characterized by N:P > 16, Si:P > 16 and Si:N < 1. The RedNano groups (RedNano I, RedNano II and RedNano III) were observed in waters with Si:P ratio above 16 and Si:N ratio equal to 1. However, RedNano I were more likely found in waters with N:P ratio above 16 while RedNano II and RedNano III were more likely found in waters characterized by a N:P ratio below 16. Finally, HsNano were observed in waters characterized by a N:P ratio below 16, a Si:P equal to 16 and a Si:N ratio above 1.

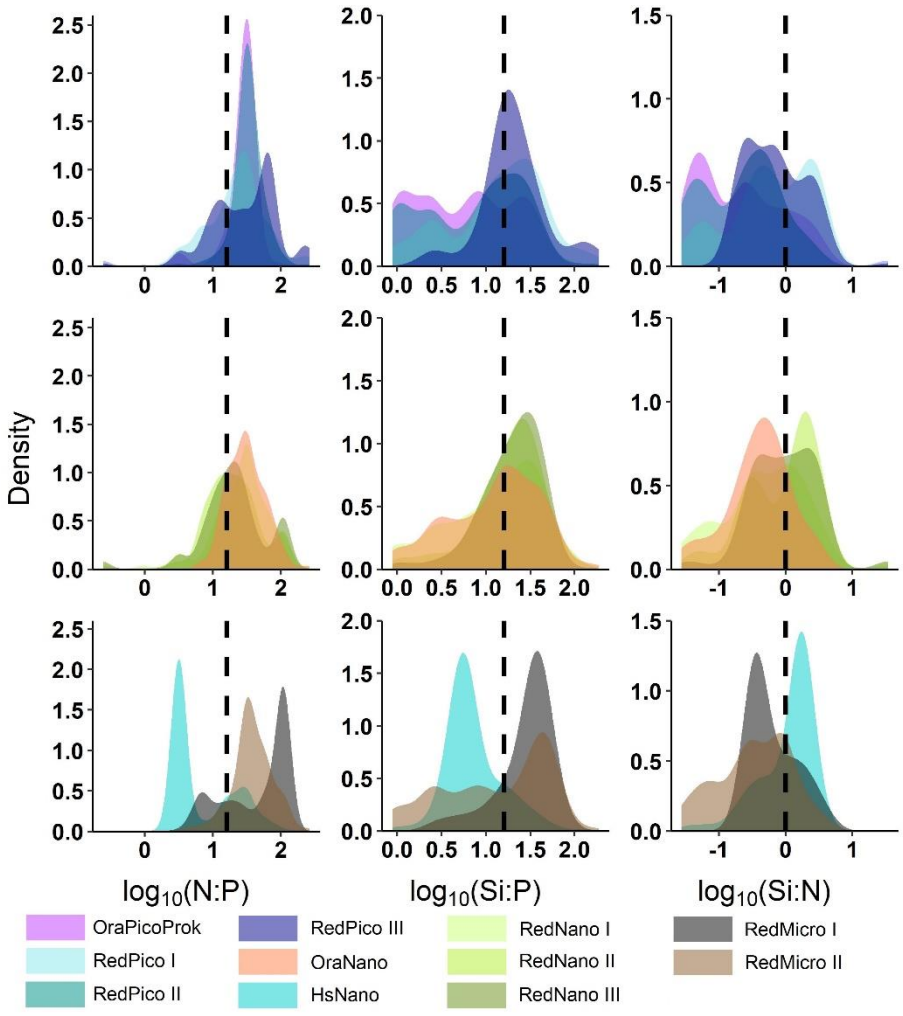

Figure 8: Kernel Density Estimation plots showing the frequency of abundance of each Phytoplankton Functional Group related to nutrient ratios (*N* = 104). The dashed lines represent the logarithm of the Redfield ratios (i.e. N:P = 16; Si:P = 16; Si:N = 1).

3.7. Niche overlap

The Schoener Index is the similarity between the niche breadth (i.e. hypervolume of n dimensions where n is the number of variables used to define the niche breadth) of two species or groups. Here, this index reveals the overlap between pairs of phytoplankton functional groups (Figure 9). The niche overlap (NOv) was comprised between 0.35 (RedMicro *I* and RedPico II) and 0.74 (OraPicoProk and RedPico II). We set arbitrary low NOv for values below 0.45, intermediate NOv for values of NOv comprised between 0.45 and 0.60, high NOv for values above 0.60. High NOv was found between three picophytoplankton groups: OraPicoProk, RedPico I and RedPico II. The same trends were found between RedNano I and RedNano II and between RedNano II and RedNano III. In addition, HsNano exhibited high NOv with OraPicoProk and RedPico II. RedMicro II showed high NOv with all the phytoplankton groups except RedPico III (low NOv), RedNano III and RedMicro I (intermediate NOv). RedMicro I had low NOv together with picophytoplankton (OraPicoProk, RedPico I, RedPico II, RedPico III), OraNano and HsNano. RedPico III exhibited low NOv with the three other picophytoplankton groups: OraPicoProk, RedPico I and RedPico II.

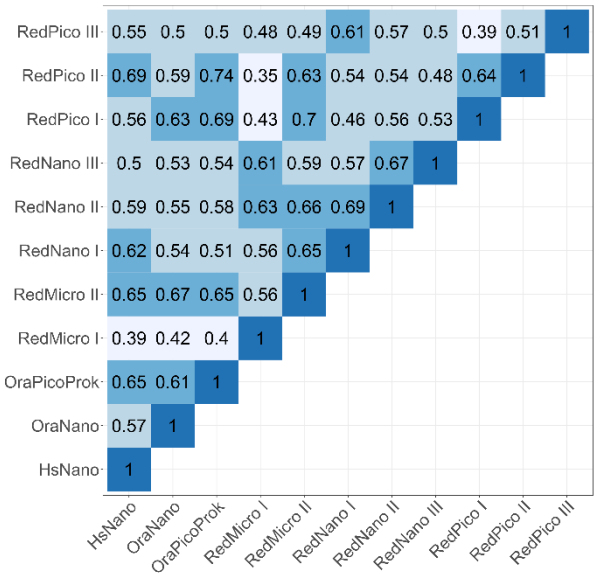

Figure 9: Upper correlation matrix representing pairwise niches overlap between the different phytoplankton functional groups defined by automated pulse shape-recording flow cytometry. Blue gradient, from light blue to dark blue, shows the increase in niche overlap given by the Schoener Index. Below 0.45, the Schoener Index is low; from 0.45 to 0.59, values are intermediate and above 0.60, values of the Schoener Index are high.

3.8. Deterministic model

The beta-regression model of the Local Contribution of each site to Beta Diversity (LCBD; derived from the abundances obtained by flow cytometry) that environmental variables explained 36% of the variation in the LCBD (table 2). A significant spatial autocorrelation was found and then considered for the analysis. Temperature and the distance to the shore explained positively and significantly ($p < 0.0001$) the values of LCBD. Intercept and salinity were negatively and significantly ($p < 0.001$) related to the LCBD values. Bathymetry was not significant. Similar to LCBD model, we found a spatial autocorrelation for SCBD model. Thus, we consider this effect for the

model. As expected, niche position was negatively and significantly related to the SCBD in our second model ($p = 0.0004$). Relation between niche breadth and SCBD was non-significant ($p = 0.27$). Consequently, the niche position of PFGs is a good estimator of the SCBD amongst the different water bodies. Despite significant variables in this latter model, the variables only explained 8% of the variance in the SCBD (table 2).

Table 2: Beta regression analysis of two responses variables: Local Contribution to Beta Diversity (LCBD) and Species Contribution to Beta Diversity (SCBD). The LCBD was explained by the continuous environmental data. The SCBD was explained by the PFG niche features (niche position and niche breadth). SE: Standard Error, df: degree of freedom, z: z-statistic (estimate divided by SE) and p: probability-value. Fixed effects were added in each model to account for spatial autocorrelation. Fixed effects for LCBD model were represented by latitude and longitude while fixed effects for SCBD model were represented by the water bodies.

	Estimate	SE	df	z	p-value	Pseudo-R^2
(a) LCBD						
Intercept	-7.09	0.56	8	-12.60	<0.0001	
Temperature	0.23	0.01	8	15.75	<0.0001	
Salinity	-0.08	0.01	8	-6.52	<0.0001	
Distance to shore	0.01	0.004	8	16.10	<0.0001	
Bathymetry	0.001	0.0009	8	-.013	0.89	
Fixed: intercept	39.23	3.38	8	11.63	<0.0001	
Fixed: Latitude	-0.59	0.067	8	-8.86	<0.0001	
Fixed: Longitude	0.30	0.043	8	7.02	<0.0001	0.36
(b) SCBD						
Intercept	-1.91	0.22	5	-9.88	<0.0001	
Niche position	-12.33	3.48	5	-2.65	0.0004	
Niche breadth	-0.45	0.41	5	-0.42	0.27	
Fixed: intercept	2.57	0.33	5	7.76	<0.0001	
Fixed: Water Body	-0.13	0.06	5	-2.07	0.039	0.08

4. Discussion

The present work reports the first trial on the relevance of applying a functional approach of phytoplankton beta-diversity and its relation to phytoplankton ecological niches at high spatial and temporal resolution in the eastern English Channel and southern North Sea. The functionality of phytoplankton was obtained using the optical traits derived from an automated flow cytometer which permitted to address the whole phytoplankton size-range at high spatial (one measure every c.a. 1.5 km according to the R.V. speed) and high temporal resolutions (one measure every 10 min). Covering such spatial area at successive period was only possible by joint international cross-border collaborations within local, national and European observation networks and projects.

4.1. Local and Species Contribution to beta-Diversity

4.1.1. Spatiotemporal dynamics

To our knowledge, we applied for the first time the LCBD to the functional groups instead of taxa as currently carried out by previous studies. Here, the LCBD confirmed the spatiotemporal heterogeneity in the PFGs distribution observed from the abundance (Figure 3). Therefore, it demonstrated the efficiency of coupling LCBD to high frequency PFGs datasets acquired by automated flow cytometry. In addition, the LCBD showed functional community changes due to the less abundant PFGs. The biggest and most significant changes in community composition were more likely observed in coastal areas, under freshwater influence, mainly represented by the alternance in dominance between picophytoplankton versus nanophytoplankton and microphytoplankton size classes even though high LCBD were also found at the farthest location from the coast in the North Sea following high HsNano abundance. In our study, the fact that all NanoFLR and microphytoplankton groups contributed more to the total abundance as the distance to the coast decreased in areas under freshwater influence was consistent with the theory of enrichment (Riebesell 1974). From the other nanoeukaryote groups, the distribution of HsNano abundance increased with the distance to the coast in the SNS, forming high abundance patches in central North Sea waters close to the Dogger Bank, as previously described by Charalampopoulou et al. (2011). These observations are particularly congruent as the distance to the shore (Baretta-Bekker et al. 2009) and the salinity (Desmit et al. 2015) were evidenced as structuring features for plankton. Both parameters are well correlated with nutrients because high nutrient concentrations are brought by a variety of freshwater inputs due to river as well as land disperse runoff (Ruddick and Lacroix 2006) compared to low but constant inputs of the Atlantic Ocean. The bottleneck effect of the Dover Strait contributed to drive Atlantic waters to the southern North Sea through the English Channel resulting in spatial heterogeneity of hydrological and physico-chemical parameters as well as bacteria, phytoplankton and zooplankton communities (Aubert et al. 2022). These hydrological effects combined to the number of estuaries result in a well-marked separation between brackish water formed by rivers run-offs and offshore mid-Channel Atlantic waters, both flowing northwards. Brackish-salty waters boundary is marked by a tidal front in which brackish waters from the "Coastal flow" in the EEC (Brylinski and Lagadeuc 1990) and the "Coastal river" in the SNS (Baretta-Bekker et al. 2009) structuring phytoplankton according their size, abundance and their biomass (Bonato et al. 2015).

4.1.2. LCBD—Water bodies model

Although the local environmental and spatial variables significantly explained sites contribution to β-diversity, the explaining variables of our model did not strongly explain the LCBD (table 2; R^2 adj.LCBD = 36%). To our knowledge, there is currently no study linking the functional diversity with the LCBD. However, it is possible to compare our results with few studies which have explored taxonomical diversity and LCBD relationships on invertebrates (Heino and Grönroos 2017) or zooplankton (Brito et al. 2020). The comparison between the R^2 adj.LCBD of the previous studies (Heino and Grönroos 2017; Brito et al. 2020) and ours suggests a variable relation between the β-diversity index and environmental factors. Such variable relation may be explained by the relevance of the set of environmental variables used to model the LCBD. Indeed, in (Heino and Grönroos 2017) and (Brito et al. 2020), the variables used in the model were known as structuring for the invertebrates and zooplankton, while in our study salinity and the distance to the coast are not known to be main structuring variables for marine phytoplankton whereas temperature is known to regulate only some species, such as *P. globosa* in our case (Verity et al. 1988). However, as the scope of our study concerned only coastal phytoplankton communities,

salinity and temperature were expected to be structuring variables for the abundance of our PFGs. The high LCBD values were indeed observed under low salinity and high temperature revealing the nearshore-offshore dilution of the freshwater inputs (Figure 4B; supp. table 1). Despite the high correlation of salinity and nutrients acquired at low frequency (Desmit et al. 2015), considering nutrient data at high spatial resolution would have certainly increased the relevance of the model. Monitoring the nutrient at high resolution should be applied in our study area representing a major improvement in studying small scales processes affecting phytoplankton (Vuillemin et al. 2009; Hydes et al. 2010; Pellerin et al. 2016). In this way, recent developments of in situ nutrient sensors (e.g. wet chemical analyzers, UV optical sensors and electrochemical sensors) are promising (Daniel et al. 2020).

4.2. High frequency automated flow cytometry

The automated flow cytometer permitted to report short-term spatiotemporal dynamic of phytoplankton at a functional level. While the overall dynamic resulted in the alternation between the size fractions of phytoplankton following to the hydrology such as picophytoplankton versus nanophytoplankton and microphytoplankton (Bonato et al. 2015; Thyssen et al. 2015; Aardema et al. 2019), the high frequency permitted to detect shifts of subsidiary phytoplankton groups. These fast changes in phytoplankton communities suggest a patchiness structure organized at the sub-mesoscale (Louchart et al. 2020b).

The most stricking alternation between phytoplankton functional groups is certainly the spatial segregation between picophytoplankton, including *OraPicoProk* and picoeukaryotes, and nanoeukaryotes and microphytoplankton in terms of abundance. This observation relies on the origin of physico-chemical inputs that intensifies the ecological contrasts from the nearshore-offshore gradients associated to the distance to estuaries. While the high abundance of *OraPicoProk* and picophytoplankton groups along the English coasts, Thames estuary and offshore waters of the southern North Sea implies the intrusion of Atlantic waters (Ruddick and Lacroix 2006; Desmit et al. 2015), the high abundance along the southern French coasts of the eastern English Channel and along Belgian and Dutch coastal waters is more typical of a post-bloom assemblage which usually happens in late spring/early summer in the Bay of Seine and offshore waters of the English Channel (Napoléon et al. 2014). Along the English coasts and offshore waters of the Dover Strait, the high abundance of *OraPicoProk* and picophytoplankton showed by our study was also confirmed by the complementary survey of Aubert et al. (2022). Even though microphytoplankton represented up to 80% of the total phytoplankton biomass, the low absolute biomass values found in the Bay of Seine by the complementary study of Louchart et al. (2020a) also suggested a starting bloom of diatoms in this area. On the other hand, the fact that the diatom *Pseudo-nitzschia* (RedMicro I) was co-dominating the PFGs with *Phaeocystis globosa* (RedNano) at the vicinity of the Scheldt-Rhine-Meuse ROFI marked probably the last phase of the spring bloom around the mid of May and in which *P.-nitzschia* colonizes *P. globosa* colonies (Sazhin et al. 2007).

Among nanoeukryotes, the calm conditions on the most offshore waters of the North Sea were suitable with the establishment and developpement of high abundance of HsNano (Charalampopoulou et al. 2011). The absence of OraNano or at least their low abundance is congruent with the theory that they occur after a disturbance of the environment (high turbulence and nutrient depleted conditions; Schapira et al. 2008). The change of abundance between the RedNano I, RedNano II and RedNano III representing the different life-stages of *P. globosa* (respectively haploid and diploid free cells and colonial cells; Peperzak 1993; Rutten et al. 2005; Guiselin 2010).

The presence of RedMicro I (*Pseudo-nitzschia*) and RedMicro II (microphytoplankton) confirms the spring blooms situation.

The two spatial overlapped areas emphasized the timing of the spring blooms in the study area. During the first spatial overlap realized (PHYCO cruise (20 to 21 of April) and the VLIZ cruise (8 to 9 of May)), the abundance of the RedNano II (diploid and very fluorescent morphotype of *P. globosa*) increased. Such observation might have represented the expansion phase of the bloom in which diploid highly fluorescent morphotype evolves to the colonial morphotype (Rousseau et al. 2007). In addition, at the end of the PHYCO cruise, the colonial life-stage of *P. globosa* (RedNano III) was also co-occurring with the diploid morphotype in the French coastal waters of the "Coastal flow" supporting this hypothesis. This observation suggests the peak of the *P. globosa* bloom to have occurred in this area at the end of April. During the second spatial overlap (in the western Scheldt-Rhine-Meuse ROFI), the diploid and high fluorescent morphotype dominated the total RedNano abundance on the first recording while six days later, the second recording in the ROFI area was marked by a dominance of the haploid and low fluorescent morphotype. This latter observation in combination with the absence of the diploid morphotype relate the senescence of *P. globosa* bloom in the mid of May (Rousseau et al. 2007).

4.3. PFGs characteristics

4.3.1. Niche distribution and overlap

The application of the functional approach to the ecological niches through the use of flow cytometry represented the second innovative aspect developed in this survey. The differences in niche position and niche tolerance of phytoplankton functional groups resulted in differences on the niche overlap between them (Figure 9). These differences were due to the environmental parameters acquired at high frequency, e.g. temperature, salinity, distance to shore and bathymetry. The residual tolerances calculated in our study ranged between 28% and 86%. Other factors should have been considered to strengthen the results such as chemical (e.g. nutrients), physical (e.g. turbulence, PAR, light attenuation, currents, wind stress) or physiological/biological factors (e.g. photosynthetic parameters, competition, parasitism, predation, viral lysis). Other studies focusing on low frequency discrete long-term sampling connecting phytoplankton species with nutrients found residual tolerances in the same range as our study (15% to 94% in Heino and Soininen (2006); 55% to 87% in Hernández Fariñas et al. (2015); 46% to 84% in Karasiewicz et al. (2018)). Consequently, adding some structuring variables such as nutrients might not have provided better explanation of the niche parameters.

Similarly to Houliez et al. (2021), our study found that the marginality (i.e. niche position) and the tolerance (i.e. niche breadth) could be extended to the spatial distribution of the PFGs. Here, the variables explained between 12.4% and 55.2% of the inertia of the PFGs. Concretely, widespread PFGs such as two out of three life stages of *P. globosa* (RedNano II and RedNano III) exhibited the lowest marginality meaning their niche was wide during the spring period considered, thus exhibiting a large spatial distribution. This observation was recently confirmed for the Belgian waters (Aubert et al. 2022). At the opposite, RedPico III, HsNano and *Pseudo-nitzschia* occurred in few sites exhibiting high marginality. This means that a marginal PFG is spatially restricted to small areas. In our study, their distribution is highly patchy. In addition, widespread PFGs were also observed to be more tolerant to environment changes than the spatially restricted PFGs which were more constraint by the environment defined in this study.

Niche parameters obtained from the present study are inferred to the timescale of *P. globosa* bloom of 2017. Therefore, our finding probably does not reflect the yearly ecological niches in the area. The view of the bloom presented here would probably have missed short-term events such as positive and negative growth (i.e. fitness) of populations. This limitation is often found in niche estimation through OMI analysis as studies consider interannual data. We suggest for future analysis at such scale to refine the view provided by the OMI by completing it by the Optimal Niche Estimate (Grüner et al. 2011) to consider the fitness within the populations.

The spatial segregation of the PFGs can be used to explain the coastal ecosystem classification (Cebrián and Valiela 1999) of the eastern English Channel and southern North Sea. The French EEC coast was marked by low overlap values between RedMicro II and *Pseudo-nitzschia* on one side and *Phaeocystis globosa* on the other side and resulting of the features of an Enclosed Coastal Ecosystem (ECE, Bonato et al. 2015), a succession from late winter to late spring by microphytoplankton (mainly diatoms) and by nanophytoplankton especially *P. globosa* (e.g. Schapira et al. 2008). At the opposite, the Atlantic waters flowing towards the northeast in the English Channel are forming the offshore waters of both the English Channel and the southern North Sea as well as the English coastal waters of the EEC. These areas can be considered as Open Coastal Ecosystem (OCE, Bonato et al. 2015). Picophytoplankton (i.e. *OraPicoProk*, RedPico I, RedPico II and RedPico III) dominates such ecosystems. Because the water bodies of the English Channel are drifting towards the North Sea, the ECE defines a continuum of brackish waters from the Bay of Seine to the Wadden Islands (Desmit et al. 2015), interrupted by some temporal and spatial discontinuities, as in the Haute Normandy coasts and southern part of the Belgian Coastal Zone which are both OCE. At present, this classification in coastal ecosystems only focused on the bloom period in the study area and requires to be extended to the different seasons to fully reflect the hydrology and plankton communities of the study area.

Low overlap values between RedMicro II and *Pseudo-nitzschia* groups versus *P. globosa* life-stages are supported by the phenology of the blooms. In spring, the timing and the amplitude of the blooms are strongly dependent of the nutrient stock and the light availability. This result is also supported by the high abundance of the different life-stages of *P. globosa* along the coast (Lancelot et al. 1987). The relatively higher niche overlap between *P. globosa* and *Pseudo-nitzschia* spp. reveals a spatiotemporal co-occurrence of the two groups. Some differences highlighted by the N:P and Si:N ratios showed that niches of single-cell stages of *P. globosa* and *Pseudo-nitzschia* spp. are different. However, the colonial stage of *P. globosa* and *Pseudo-nitzschia* spp. share the same nutrient niche revealing that *P. globosa* and *Pseudo-nitzschia* spp. co-occur in space. This observation is supported by the fact that during the transition between the *P. globosa* single-cell to the colonial stage and when colonies are of a sufficient size, *Pseudo-nitzschia* can use *P. globosa* as habitat (Sazhin et al. 2007). Despite results perfectly consistent with classical observations in the study area, our rationale must be interpreted with caution as similarity and equivalency tests for niche overlap could not be performed.

4.3.2. SCBD—niches parameter model

Our findings across water bodies highlight that Species Contribution to β-diversity (SCBD) considering Phytoplankton Functional Groups (PFGs) depends on the abundance of the PFGs as well as their niche characteristics. We found negative and significant relation between the SCBD and the niche position and positive but weak relation between SCBD and niche breadth. This result agrees with previous studies showing that, at sub-regional scales, niche position is better than niche breadth to address the contribution of the PFGs to the β-diversity

(Heino and Grönroos 2014; Tonkin et al. 2016). Nevertheless, our model performed weaker relation between the niche position and SCBD than other studies (Heino and Grönroos 2017; da Silva et al. 2018). We speculate that the difference may be related to two reasons which may be explored in a future survey. First, our consideration of niche characteristics is limited by the temporal extent of the measurements. The present survey only targeted the spring productive period (i.e. the bloom) which missed other productive periods as well as the non-productive periods, corresponding mainly to June to early-March. Extreme values of temperature and salinity occurring in winter and summer periods must have considerably changed the niche size. Furthermore, niche characteristics are also limited by the number of structural environmental parameters. In the eastern English Channel and southern North Sea, nutrients, currents, fronts are among the most important parameters in phytoplankton community structure and distribution affecting niches size (Karasiewicz et al. 2018). The weak relationship suggests stronger relation between PFGs and their SCBD by connecting additional intrinsic parameters of the PFGs to the model. Indeed, despite traits importance remained discussed (da Silva et al. 2018) or minored in comparison to niche characteristics (Heino and Grönroos 2014, 2017), they have been related to SCBD (Heino and Grönroos 2017). However, traits strongly support phytoplankton community's structure (Litchman et al. 2007). Consequently, as the optical properties derived from the PFGs can be assimilated to optical traits (Fragoso et al. 2019), we assume the CytoSense may represent a unique opportunity for future investigation of the relation between PFGs characteristics (traits-niche) and the SCBD using *in situ* data.

Understanding the key determinants to LCBD and SCBD is important for community ecology as well as ecosystems' management. However, only LCBD has been explored in the past for the purpose of plankton management (Rombouts et al. 2019). As niche is found as a good predictor of the SCBD of the PFGs, we are now able to relate more precisely how the PFGs can evolve in changing environmental conditions at local scales and over short-term periods. From a management perspective, the relationship between niche and SCBD would therefore help understanding which environmental condition is better to target to impact the development of some taxa or phytoplankton group. This is particularly crucial in the management of harmful algae to reduce the amplitude and the timing of their blooms. At larger scales (regional or broad scale), the application of this methodology to long-term plankton monitoring may provide better explanation how pressures such as eutrophication and climate change can act within each species of the plankton communities. We may therefore be able to predict their development in the context of broad scale environmental changes.

Conclusion

High spatio-temporal variability of phytoplankton community, defined by their functional diversity, was studied during the spring bloom in the eastern English Channel and southern North Sea. The patchiness in phytoplankton distribution resulted from dynamic environmental conditions. As a consequence, the patchiness segregation of the phytoplankton functional groups (PFGs) was successfully highlighted by connecting the concept of the niche to phytoplankton groups discriminated by flow cytometry. While cruising over the eastern English Channel and southern North Sea, changes in community composition and the contribution of each PFG occurred. Both were modeled by β-diversity indices (LCBD and SCBD), applied to functional groups, which could be predicted by environmental conditions and intrinsic parameter of each PFG. We demonstrated that the application of the SCBD to the PFGs is ecologically relevant. Future investigations should therefore include modeling β-diversity indices to report and then predict plankton communities' evolution and the contribution of each plankton unit by linking

ecological features (niche and traits) and pressures at both short-term (e.g. extreme event such as strong, precipitations) by using automated optical high resolution definition of PFGs and long term (e.g. climate change) by using traditional approaches.

In Europe, management of marine waters is supported by the member states of the OSPAR commission through the MSFD. This directive connects the ICG-COBAM (OSPAR) Pelagic Habitat Indicator (PH1/FW5 "changes in plankton lifeforms", PH2 "changes in plankton biomass/abundance" and PH3 "changes in plankton diversity"; Budria et al. (2017); Rombouts et al. (2019); Bedford et al. (2020)) to both abiotic and biotic parameters to better understand the environmental status of marine ecosystems. As β-diversity indices are part of the methodology of the ICG-COBAM PH3, we strongly support the fact that automated flow cytometry mounted onboard research vessels and/or ships-of-opportunity could be a powerful tool for investigating pelagic habitats at high spatial and temporal resolution, where traditional fixed monitoring stations could not properly assess marine waters. Furthermore, this approach represents, by its large size-range of particles recorded, a unique tool to investigate the pairs picoeukaryotes versus nanoeukaryotes and microphytoplankton which informs about the trophic state of a habitat. In this purpose, current collaborative initiatives within European projects (i.e. H2020 INFRAIA JERICO-S3) as well as developing regular monitoring of offshore waters will add offshore view of the ICG-COBAM Pelagic Habitat indicators across the large-spatial areas.

Acknowledgements

We thank the crew and the captains of the research vessels *Côtes de la Manche* (CNRS INSU), *Simon Stevin* (VLIZ) and *Zirfaea* (RWS), as well as the scientific and technical staff of the different institutes involved (LOG, VLIZ and RWS). We also thank the P.I. of the Belgian (until 2016 Lennert Tyberghein, VLIZ) and Dutch (Arnold Veen, RWS) cruises. We are thankful to Dr. Fernando Gomez (University of Salento) for carrying the microscopy counts of the PHYCO cruise and his remarks on this manuscript. We are thankful to Eric Lécuyer for ammonia analysis of the PHYCO cruise.

Author contribution

AL, FL, ED, JM, MR, KD, FGS and LFA conceived this study. LFA coordinated the sampling and measurements onboard the *Côtes de la Manche* (CNRS-INSU). ED and KD planned and performed the VLIZ-Cruise. JM coordinated the sampling and measurements onboard the *Simon Stevin* (VLIZ). MR coordinated the sampling and measurements onboard the *Zirfaea* (RWS). AL, FL, JM, MR and LFA were involved in the sampling and measuring onboard. AL carried out flow cytometry analysis and ran the statistical analysis. MC and EL carried out the nutrient analysis of the PHYCO-Cruise. AL wrote the manuscript draft and integrated all comments and suggestions in the different versions. FA, FL and MC performed a deep revision and improvement of the manuscript. All authors contributed to proofread and to validate the final version of the manuscript. We also thanks the three anonymous reviewers for their constructive comments.

Funding

AL was co-funded by a PhD grant from the "Université du Littoral-Côte d'Opale" co-funded by a "Hauts-de-France" Regional research fellowship from October 2016 to September 2019. He was also funded from January 2020 to October 2020 by a research fellowship grant of PON PLaCE ARS01_00891 of the Stazione Zoologica

Anton Dohrn and an IFERMER LER/BL contract from October 2020 to June 2021, and he is at present funded by a CNRS research fellowship in the frame of the EMFF project NEA PANACEA (grant number 110661/2020/839628/SUB/ENV.C.2) This work has been financially supported by the European Union (ERDF), the French State, the French Region Hauts-de-France and IFREMER, in the framework of the project CPER MARCO 2015-2021. PHYCO-cruise was funded by the JERICO-NEXT project and MEMM/MTES-CNRS/INSU convention for the MSFD and Monitoring Programme implementation in Pelagic Habitats of France. The VLIZ cruise was funded by the JERICO–NEXT project and data was provided as part of the Flemish contribution to the LifeWatch ESFRI by the Flanders Marine Institute (VLIZ). The RWS cruise was also funded by the JERICO-NEXT project. The JERICO-NEXT project has received funding from the European Union's Horizon 2020 research and innovation programme under grant agreement no. 654410.

Data availability

The PSFCM dataset generated during the current study is available from the corresponding authors on reasonable request. Nutrient dataset from the JERICO-NEXT/LifeWatch VLIZ cruise is available through the Marine Data Archive (http://mda.vliz.be/) and the LifeWatch Data explorer (http://www.lifewatch .be/en/lifewatch-data-explorer). Nutrient and microscopy counts datasets from the MWTL RWS cruise were provided by the Dutch Ministry of Intrastructure and Watermanagment and available at: https://waterinfo.rws.nl/. Environmental as well as phytoplankton-related data of the PHYCO cruise will be made available in the SISMER database of France Cruises (https://doi.org/10.17600/17010500).

Declarations

Conflict of interest

The authors have no conflicts of interest to declare that are relevant to the content of this article.

Ethical approval

Not applicable

Consent to participate

Not applicable

Consent for publication

Not applicable

References

Aardema HM, Rijkeboer M, Lefebvre A, Veen A, Kromkamp JC (2019) High-resolution underway measurements of phytoplankton photosynthesis and abundance as an innovative addition to water quality monitoring programs. Ocean Science 15:1267–1285. doi: 10.5194/os-15-1267-2019

Aminot A, Kérouel R (2004) Hydrologie des écosystèmes marins: paramètres et analyses. IFREMER

Aubert A, Beauchard O, Blok RD, Artigas LF, Sabbe K, Vyverman W, Amadei Martínez L, Deneudt K, Louchart A, Mortelmans J, Rijkeboer M, Debusschere E (2022) From Bacteria to Zooplankton : An Integrative Approach Revealing Regional Spatial Patterns During the Spring Phytoplankton

Bloom in the Southern Bight of the North Sea. Frontiers in Marine Science 9:1–20. doi: 10.3389/fmars.2022.863996

Baretta-Bekker JG, Baretta JW, Latuhihin MJ, Desmit X, Prins TC (2009) Description of the long-term (1991-2005) temporal and spatial distribution of phytoplankton carbon biomass in the Dutch North Sea. Journal of Sea Research 61:50–59. doi: 10.1016/j.seares.2008.10.007

Bedford J, Ostle C, Johns DG, Atkinson A, Best M, Bresnan E, Machairopoulou M, Graves CA, Devlin M, Milligan A, Pitois S, Mellor A, Tett P, McQuatters-Gollop A (2020) Lifeform indicators reveal large-scale shifts in plankton across the North-West European shelf. Global Change Biology 26:3482–3497. doi: 10.1111/gcb.15066

Bonato S, Christaki U, Lefebvre A, Lizon F, Thyssen M, Artigas LF (2015) High spatial variability of phytoplankton assessed by flow cytometry, in a dynamic productive coastal area, in spring: The eastern English Channel. Estuarine, Coastal and Shelf Science 154:214–223. doi: 10.1016/j.ecss.2014.12.037

Bonato S, Breton E, Didry M, Lizon F, Cornille V, Lécuyer E, Christaki U, Artigas LF (2016) Spatio-temporal patterns in phytoplankton assemblages in inshore-offshore gradients using flow cytometry: A case study in the eastern English Channel. Journal of Marine Systems 156:76–85. doi: 10.1016/j.jmarsys.2015.11.009

Breton E, Brunet C, Sautour B, Brylinski J-M (2000) Annual variations of phytoplankton biomass in the Eastern English Channel: comparison by pigment signatures and microscopic counts. Journal of Plankton Research 22:1423–1440. doi: 10.1093/plankt/22.8.1423

Breton E, Christaki U, Bonato S, Didry M, Artigas LF (2017) Functional trait variation and nitrogen use efficiency in temperate coastal phytoplankton. Marine Ecology Progress Series 563:35–49. doi: 10.3354/meps11974

Brito MT da S, Heino J, Pozzobom UM, Landeiro VL (2020) Ecological uniqueness and species richness of zooplankton in subtropical floodplain lakes. Aquatic Sciences 82:1–13. doi: 10.1007/s00027-020-0715-3

Broennimann O, Fitzpatrick MC, Pearman PB, Petitpierre B, Pellissier L, Yoccoz NG, Thuiller W, Fortin MJ, Randin C, Zimmermann NE, Graham CH, Guisan A (2012) Measuring ecological niche overlap from occurrence and spatial environmental data. Global Ecology and Biogeography 21:481–497. doi: 10.1111/j.1466-8238.2011.00698.x

Brunet C, Lizon F (2003) Tidal and diel periodicities of size-fractionated phytoplankton pigment signatures at an offshore station in the southeastern English Channel. Estuarine, Coastal and Shelf Science 56:833–843. doi: 10.1016/S0272-7714(02)00323-2

Brussaard CPD, Gast GJ, Van Duyl FC, Riegman R (1996) Impact of phytoplankton bloom magnitude on a pelagic microbial food web. Marine Ecology Progress Series 144:211–221. doi: 10.3354/meps144211

Brylinski J-M (1991) Le “fleuve cotier” : un phenomene hydrologique important en Manche orientale (exemple du Pas-de-Calais). Oceanol Acta 11:197–203.

Brylinski JM, Lagadeuc Y (1990) L’interface eaux côtières/eaux du large dans le Pas-de-Calais (côte française) : une zone frontale. Comptes rendus de l’Académie des Sciences 311:535–540.

Brylinski JM, Brunet C, Bentley D, Thoumelin G, Hilde D (1996) Hydrography and phytoplankton biomass in the Eastern English Channel in spring 1992. Estuarine, Coastal and Shelf Science 43:507–519. doi: 10.1006/ecss.1996.0084

Budria A, Aubert A, Rombouts I, Ostle C, Atkinson A, Widdicombe C, Goberville E, Artigas F, Johns D, Padegimas B, Corcoran E, McQuatters-Gollop A (2017) Cross linking plankton indicators to better define GES of pelagics habitats. In: EcApRHA Deliverable, WP1.4. OSPAR Commission, p 54

Cebrián J, Valiela I (1999) Seasonal patterns in Phytoplankton in coastal ecosystems. Journal of Plankton Research 21:429–444.

Chacón JE, Duong T (2018) Multivariate Kernel Smoothing and Its Applications, 1st Ed. Chapman and Hall, New York

Charalampopoulou A, Poulton AJ, Tyrrell T, Lucas MI (2011) Irradiance and pH affect coccolithophore community composition on a transect between the North Sea and the Arctic Ocean. Marine Ecology Progress Series 431:25–43. doi: 10.3354/meps09140

Costanza R, D'Arge R, De Groot R, Farber S, Grasso M, Hannon B, Limburg K, Naeem S, O'Neill RV, Paruelo J, Raskin RG, Sutton P, Van Den Belt M (1997) The value of the world's ecosystem services and natural capital. Nature 387:253–260. doi: 10.1038/387253a0

Cribari-Neto F, Zeileis A (2010) Beta Regression in R. Journal of Statistical Software 34:1–24. doi: 10.18637/jss.v034.i02

Cullen J, Franks P, Karl D, Longhurst A (2002) Physical influences on marine ecosystem dynamics.

da Silva PG, Medina Isabel MI, Heino J (2018) Disentangling the correlates of species and site contributions to beta diversity in dung beetle assemblages. Diversity and Distributions 24:1674–1686. doi: 10.1111/ddi.12785

Daniel A, Laës-Huon A, Barus C, Beaton AD, Blandfort D, Guigues N, Knockaert M, Munaron D, Salter I, Woodward EMS, Greenwood N, Achterberg EP (2020) Toward a Harmonization for Using in situ Nutrient Sensors in the Marine Environment. Front Mar Sci 6:773. doi: 10.3389/fmars.2019.00773

Derot J, Schmitt FG, Gentilhomme V, Zongo SB (2015) Long-term high frequency phytoplankton dynamics , recorded from a coastal water autonomous measurement system in the eastern English Channel. Continental Shelf Research 109:210–221. doi: 10.1016/j.csr.2015.09.015

Desmit X, Ruddick K, Lacroix G (2015) Salinity predicts the distribution of chlorophyll a spring peak in the southern North Sea continental waters. Journal of Sea Research 103:59–74. doi: 10.1016/j.seares.2015.02.007

Dolédec S, Chessel D, Gimaret-Carpentier C (2000) Niche separation in community analysis: A new method. Ecology 81:2914–2927. doi: 10.1890/0012-9658(2000)081[2914:NSICAA]2.0.CO;2

Dray S, Dufour A-B (2007) The ade4 Package: Implementing the Duality Diagram for Ecologists. Journal of Statistical Software 22:1–20. doi: 10.18637/jss.v022.i04

Dray S, Bauman D, Blanchet G, Borcard D, Clappe S, Guénard G, Jombart T, Larocque G, Legendre P, Madi N, Wagner HH (2022) adespatial: Multivariate Multiscale Spatial Analysis. Journal of Statistical Software 103:1–26. doi: 10.18637/jss.v103.i07

Dubelaar GBJ, Gerritzen PL, Beeker AER, Jonker RR, Tangen K (1999) Design and first results of CytoBuoy: A wireless flow cytometer for in situ analysis of marine and fresh waters. Cytometry 37:247–254.

Dugenne M, Thyssen M, Nerini D, Mante C, Poggiale JC, Garcia N, Garcia F, Grégori GJ (2014) Consequence of a sudden wind event on the dynamics of a coastal phytoplankton community: An insight into specific population growth rates using a single cell high frequency approach. Frontiers in Microbiology 5:1–14. doi: 10.3389/fmicb.2014.00485

Fontana S, Jokela J, Pomati F (2014) Opportunities and challenges in deriving phytoplankton diversity measures from individual trait-based data obtained by scanning flow-cytometry. Frontiers in Microbiology 5:1–12. doi: 10.3389/fmicb.2014.00324

Fontana S, Thomas MK, Moldoveanu M, Spaak P, Pomati F (2018) Individual-level trait diversity predicts phytoplankton community properties better than species richness or evenness. ISME Journal 12:356–366. doi: 10.1038/ismej.2017.160

Fragoso GM, Poulton AJ, Pratt N, Johnsen G, Purdie DA (2019) Trait-based analysis of subpolar North Atlantic phytoplankton and plastidic ciliate communities using automated flow cytometer. Limnology and Oceanography 64:1–16. doi: 10.1002/lno.11189

Gaston KJ, Blackburn TM (2007) Pattern and process in macroecology.

Gaston KJ, Blackburn TM, Lawton JH (1997) Interspecific Abundance-Range Size Relationships: An Appraisal of Mechanisms. The Journal of Animal Ecology 66:579. doi: 10.2307/5951

Grattepanche JD, Breton E, Brylinski JM, Lecuyer E, Christaki U (2011) Succession of primary producers and micrograzers in a coastal ecosystem dominated by Phaeocystis globosa blooms. Journal of Plankton Research 33:37–50. doi: 10.1093/plankt/fbq097

Grüner N, Gebühr C, Boersma M, Feudel U, Wiltshire KH, Freund JA (2011) Reconstructing the realized niche of phytoplankton species from environmental data: fitness versus abundance approach: Realized niche: fitness versus abundance. Limnol Oceanogr Methods 9:432–442. doi: 10.4319/lom.2011.9.432

Guiselin N (2010) Etude de la dynamique des communautés phytoplanctoniques par microscopie et cytométrie en flux, en eaux côtière de la Manche orientale. 237. doi: 10.1021/ie0712941

Heino J (2005) Positive relationship between regional distribution and local abundance in stream insects : a consequence of niche breadth or niche position ? Ecography 28:345–354.

Heino J, Grönroos M (2014) Untangling the relationships among regional occupancy, species traits, and niche characteristics in stream invertebrates. Ecology and Evolution 4:1931–1942. doi: 10.1002/ece3.1076

Heino J, Grönroos M (2017) Exploring species and site contributions to beta diversity in stream insect assemblages. Oecologia 183:151–160. doi: 10.1007/s00442-016-3754-7

Heino J, Soininen J (2006) Regional occupancy in unicellular eukaryotes: A reflection of niche breadth, habitat availability or size-related dispersal capacity? Freshwater Biology 51:672–685. doi: 10.1111/j.1365-2427.2006.01520.x

Hernández Fariñas T, Bacher C, Soudant D, Belin C, Barillé L (2015a) Assessing phytoplankton realized niches using a French national phytoplankton monitoring network. Estuarine, Coastal and Shelf Science 159:15–27. doi: 10.1016/j.ecss.2015.03.010

Hernández Fariñas T, Bacher C, Soudant D, Belin C, Barillé L (2015b) Assessing phytoplankton realized niches using a French national phytoplankton monitoring network. Estuarine, Coastal and Shelf Science 159:15–27. doi: 10.1016/j.ecss.2015.03.010

Houliez E, Lizon F, Thyssen M, Artigas LF, Schmitt FG (2012) Spectral fluorometric characterization of Haptophyte dynamics using the FluoroProbe: An application in the eastern English Channel for monitoring Phaeocystis globosa. Journal of Plankton Research 34:136–151. doi: 10.1093/plankt/fbr091

Houliez E, Lefebvre S, Dessier A, Huret M, Marquis E, Bréret M, Dupuy C (2021) Spatio-temporal drivers of microphytoplankton community in the Bay of Biscay: Do species ecological niches matter? Progress in Oceanography 194:102558. doi: 10.1016/j.pocean.2021.102558

Hutchinson GE (1957) Cold spring harbor symposium on quantitative biology. Concluding remarks 22:415–427.

Hydes D, Aoyama M, Aminot A, Bakker K, Becker S, Coverly S, Daniel A, Dickson AG, Grosso O, Kerouel R, van Ooijen J, Sato K, Tanhua T, Woodward EMS, Zhang JZ (2010) Determination of dissolved nutrients (N, P, Si) in seawater with high precision and inter-comparability using gas-segmented continuous flow analysers. United Nations Educational, Scientific and Cultural Organization, Paris

Karasiewicz S, Dolédec S, Lefebvre S (2017) Within outlying mean indexes: refining the OMI analysis for the realized niche decomposition. PeerJ 5:e3364. doi: 10.7717/peerj.3364

Karasiewicz S, Breton E, Lefebvre A, Hernández T (2018) Realized niche analysis of phytoplankton communities involving HAB : Phaeocystis spp . as a case study. Harmful Algae 72:1–13. doi: 10.1016/j.hal.2017.12.005

Lacroix G, Ruddick K, Ozer J, Lancelot C (2004) Modelling the impact of the Scheldt and Rhine/Meuse plumes on the salinity distribution in Belgian waters (southern North Sea). Journal of Sea Research 52:149–163. doi: 10.1016/j.seares.2004.01.003

Lancelot C, Billen G, Sournia A, Weisse T, Colijn F, Veldhuis MJW, Davies A, Wassmann P (1987) Phaeocystis blooms and nutrient enrichment in the continental coastal zones of the North Sea. Ambio 16:38–46.

Lefebvre A, Guiselin N, Barbet F, Artigas FL (2011) Long-term hydrological and phytoplankton monitoring (1992-2007) of three potentially eutrophic systems in the eastern English Channel and the Southern Bight of the North Sea. ICES Journal of Marine Science 68:2029–2043. doi: 10.1093/icesjms/fsr149

Legendre P, De Cáceres M (2013) Beta diversity as the variance of community data : dissimilarity coefficients and partitioning. Ecology Letters. doi: 10.1111/ele.12141

Litchman E, Klausmeier CA (2008) Trait-Based Community Ecology of Phytoplankton. Annual Review of Ecology, Evolution, and Systematics 39:615–639. doi: 10.1146/annurev.ecolsys.39.110707.173549

Litchman E, Klausmeier CA, Schofield OM, Falkowski PG (2007) The role of functional traits and trade-offs in structuring phytoplankton communities: Scaling from cellular to ecosystem level. Ecology Letters 10:1170–1181. doi: 10.1111/j.1461-0248.2007.01117.x

Louchart A, de Blok R, Debuschere E, Gómez F, Lefebvre A, Mortelmans J, Rijkeboer M, Deneudt K, Veen A, Wacquet G, Schmitt FG, Artigas LF (2020a) Automated techniques to follow the spatial distribution of Phaeocystis globosa and diatom spring blooms in the English Channel and North Sea . In: Hess P (ed) Harmful Algae 2018 – From Ecosystems to Socioecosystems. Proceedings of the 18th International Conference on Harmful Algae. International Society for the Study of Harmful Algae, Nantes, pp 51–55

Louchart A, Lizon F, Lefebvre A, Didry M, Schmitt FG, Artigas LF (2020b) Phytoplankton distribution from Western to Central English Channel, revealed by automated flow cytometry during the summer-fall transition. Continental Shelf Research. doi: 10.1016/j.csr.2020.104056

Lovejoy S, Currie WJS, Tessier Y, Claereboudt MR, Bourget E, Roff JC, Schertzer D (2001) Universal multifractals and ocean patchiness: phytoplankton, physical fields and coastal heterogeneity. Journal of Plankton Research 23:117–141. doi: 10.1093/plankt/23.2.117

Massicotte P, South A, Hufkens K (2023) rnaturalearth: World Map Data from Natural Earth.

Mortelmans J, Deneudt K, Cattrijsse A, Beauchard O, Daveloose I, Vyverman W, Vanaverbeke J, Timmermans K, Peene J, Roose P, Knockaert M, Chou L, Sanders R, Stinchcombe M, Kimpe P, Lammens S, Theetaert H, Gkritzalis T, Hernandez F, Mees J (2019) Nutrient, pigment, suspended matter and turbidity measurements in the Belgian part of the North Sea. Sci Data 6:22. doi: 10.1038/s41597-019-0032-7

Nagy-László Z, Padisák J, Borics G, Abonyi A, B-Béres V, Várbíró G (2020) Analysis of niche characteristics of phytoplankton functional groups in fluvial ecosystems. Journal of Plankton Research 42:355–367. doi: 10.1093/plankt/fbaa020

Napoléon C, Fiant L, Raimbault V, Riou P, Claquin P (2014) Dynamics of phytoplankton diversity structure and primary productivity in the English Channel. Marine Ecology Progress Series 505:49–64. doi: 10.3354/meps10772

Pellerin BA, Stauffer BA, Young DA, Sullivan DJ, Bricker SB, Walbridge MR, Clyde GA, Shaw DM (2016) Emerging Tools for Continuous Nutrient Monitoring Networks: Sensors Advancing Science and Water Resources Protection. Journal of the American Water Resources Association 52:993–1008. doi: 10.1111/1752-1688.12386

Peperzak L (1993) Daily irradiance governs growth rate and colony formation of <i>Phaeocystis<\i> (Prymnesiophyceae). Journal of Plankton Research 15:809–821. doi: 10.1093/plankt/15.7.809

Pereira GC, Figueiredo AR, Ebecken NFF (2018) Using in situ flow cytometry images of ciliates and dinoflagellates for aquatic system monitoring. Brazilian Journal of Biology 78:240–247.

Pomati F, Kraft NJB, Posch T, Eugster B, Jokela J, Ibelings BW (2013) Individual Cell Based Traits Obtained by Scanning Flow-Cytometry Show Selection by Biotic and Abiotic Environmental

Factors during a Phytoplankton Spring Bloom. PLoS ONE 8:e71677. doi: 10.1371/journal.pone.0071677

Quisthoudt C (1987) Primary production in Dover Strait (France): Spatio-temporal variations off Cap Griz-Nez. Comptes rendus de l'Académie des Sciences Paris 10:245–250.

Reynolds CS (1997) Vegetation processes in the pelagic: a model for ecosystem theory. Ecology Institute Oldendorf

Riebesell JF (1974) Paradox of Enrichment in Competitive Systems. Ecology 55:183–187.

Rombouts I, Simon N, Aubert A, Cariou T, Feunteun E, Guérin L, Hoebeke M, McQuatters-Gollop A, Rigaut-Jalabert F, Artigas LF (2019) Changes in marine phytoplankton diversity: Assessment under the Marine Strategy Framework Directive. Ecological Indicators 102:265–277. doi: 10.1016/j.ecolind.2019.02.009

Rousseau V, Chrétiennot-Dinet MJ, Jacobsen A, Verity P, Whipple S (2007) The life cycle of Phaeocystis: State of knowledge and presumptive role in ecology. Biogeochemistry 83:29–47. doi: 10.1007/978-1-4020-6214-8_4

Ruddick K, Lacroix G (2006) Hydrodynamics and meteorology of the Belgian Coastal Zone. In: Rousseau V, Lancelot C, Cox D (eds) Current status of eutrophication in the Belgian Coastal Zone. pp 1–15

Rutten TPA, Sandee B, Hofman ART (2005) Phytoplankton monitoring by high performance flow cytometry: A successful approach? Cytometry Part A 64:16–26. doi: 10.1002/cyto.a.20106

Salmaso N, Naselli-Flores L, Padisák J (2015) Functional classifications and their application in phytoplankton ecology. Freshwater Biology 60:603–619. doi: 10.1111/fwb.12520

Sazhin AF, Artigas LF, Nejstgaard JC, Frischer ME (2007) The colonization of two Phaeocystis species (Prymnesiophyceae) by pennate diatoms and other protists: A significant contribution to colony biomass. Biogeochemistry 83:137–145. doi: 10.1007/978-1-4020-6214-8_11

Schapira M, Vincent D, Gentilhomme V, Seuront L (2008) Temporal patterns of phytoplankton assemblages , size spectra and diversity during the wane of a Phaeocystis globosa spring bloom in hydrologically contrasted coastal waters. Journal of the Marine Biological Association of the United Kingdom 88:649–662. doi: 10.1017/S0025315408001306

Schoener TW (1970) Nonsynchronous Spatial Overlap of Lizards in Patchy Habitats. Ecology 51:408–418.

Sentchev A, Korotenko K (2005) Dispersion processes and transport pattern in the ROFI system of the eastern English Channel derived from a particle-tracking model. Continental Shelf Research 25:2294–2308. doi: 10.1016/j.csr.2005.09.003

Seuront L, Schmitt F, Lagadeuc Y, Schertzer D, Lovejoy S (1999) Universal multifractal analysis as a tool to characterize multiscale intermittent patterns: example of phytoplankton distribution in turbulent coastal waters. Journal of Plankton Research 21:877–822. doi: 10.1093/plankt/21.5.877

Seuront L, Vincent D, Mitchell JG (2006) Biologically induced modification of seawater viscosity in the Eastern English Channel during a Phaeocystis globosa spring bloom. Journal of Marine Systems 61:118–133. doi: 10.1016/j.jmarsys.2005.04.010

Thyssen M, Mathieu D, Garcia N, Denis M (2008) Short-term variation of phytoplankton assemblages in Mediterranean coastal waters recorded with an automated submerged flow cytometer. Journal of Plankton Research 30:1027–1040. doi: 10.1093/plankt/fbn054

Thyssen M, Alvain S, Lefèbvre A, Dessailly D, Rijkeboer M, Guiselin N, Creach V, Artigas LF (2015) High-resolution analysis of a North Sea phytoplankton community structure based on in situ flow cytometry observations and potential implication for remote sensing. Biogeosciences 12:4051–4066. doi: 10.5194/bg-12-4051-2015

Thyssen M, Grégori G, Créach V, Lahbib S, Dugenne M, Aardema HM, Artigas L-F, Huang B, Barani A, Beaugeard L, Bellaaj-Zouari A, Beran A, Casotti R, Del Amo Y, Denis M, Dubelaar GBJ, Endres S, Haraguchi L, Karlson B, Lambert C, Louchart A, Marie D, Moncoiffé G, Pecqueur D, Ribalet F, Rijkeboer M, Silovic T, Silva R, Marro S, Sosik HM, Sourisseau M, Tarran G, Van Oostende N, Zhao L, Zheng S (2022) Interoperable vocabulary for marine microbial flow cytometry. Front Mar Sci 9:975877. doi: 10.3389/fmars.2022.975877

Tonkin JD, Heino J, Sundermann A, Haase P, Jähnig SC (2016) Context dependency in biodiversity patterns of central German stream metacommunities. Freshwater Biology 61:607–620. doi: 10.1111/fwb.12728

van Etten J (2017) R Package gdistance: Distances and Routes on Geographical Grids. Journal of Statistical Software 76:1–21.

Verity PG, Villareal TA, Smayda TJ (1988) Ecological investigations of blooms of colonial Phaeocystis pouchetti. II. The role of life-cycle phenomena in bloom termination. Journal of Plankton Research 10:749–766. doi: 10.1093/plankt/10.4.749

Vuillemin R, Sanfilippo L, Moscetta P, Zudaire L, Carbones E, Maria E, Tricoire C, Oriol L, Blain S, Le Bris N, Lebaron P (2009) Continuous nutrient automated monitoring on the Mediterranean Sea using in situ flow analyser. In: Proceedings of the OCEANS 2009. Biloxi, MS, pp 1–8